creative commons
COMMONS DEED

저작자표시-비영리-변경금지 2.0 대한민국

이용자는 아래의 조건을 따르는 경우에 한하여 자유롭게

- 이 저작물을 복제, 배포, 전송, 전시, 공연 및 방송할 수 있습니다.

다음과 같은 조건을 따라야 합니다:

저작자표시. 귀하는 원저작자를 표시하여야 합니다.

비영리. 귀하는 이 저작물을 영리 목적으로 이용할 수 없습니다.

변경금지. 귀하는 이 저작물을 개작, 변형 또는 가공할 수 없습니다.

- 귀하는, 이 저작물의 재이용이나 배포의 경우, 이 저작물에 적용된 이용허락조건을 명확하게 나타내어야 합니다.
- 저작권자로부터 별도의 허가를 받으면 이러한 조건들은 적용되지 않습니다.

저작권법에 따른 이용자의 권리는 위의 내용에 의하여 영향을 받지 않습니다.

이것은 이용허락규약(Legal Code)을 이해하기 쉽게 요약한 것입니다.

Disclaimer

dCollection

연세대학교
YONSEI UNIVERSITY

[UCI]I804:11046-000000517052

Novel Methodology for Coronary Artery Disease Evaluation: From a New Imaging Technique to Deep Learning Based Quantification

Youngtaek Hong

Department of Medical Science

The Graduate School, Yonsei University

연세대학교
YONSEI UNIVERSITY

Novel Methodology for Coronary Artery Disease Evaluation: From a New Imaging Technique to Deep Learning Based Quantification

Youngtaek Hong

Department of Medical Science

The Graduate School, Yonsei University

연세대학교
YONSEI UNIVERSITY

Novel Methodology for Coronary Artery Disease Evaluation: From a New Imaging Technique to Deep Learning Based Quantification

Directed by Professor Hyuk-Jae Chang

The Doctoral Dissertation
submitted to the Department of Medical Science
the Graduate School of Yonsei University
in partial fulfillment of the requirements for the degree of
Doctor of Philosophy

Youngtaek Hong

June 2018

연세대학교
YONSEI UNIVERSITY

This certifies that the Doctoral Dissertation of Youngtaek Hong is approved.

Thesis Supervisor: Hyuk-Jae Chang

Thesis Committee Member#1: Jung Sun Kim

Thesis Committee Member#2: Jon Suh

Thesis Committee Member#3: Hae-Jeong Park

Thesis Committee Member#4: Yang Soo Jang

The Graduate School
Yonsei University

June 2018

연세대학교
YONSEI UNIVERSITY

Acknowledgments

I would like to express my sincere gratitude to everyone who has supported, encouraged, and motivated me over the course of my Ph. D.

To begin with, I would like to express my special appreciation and thanks to my advisor *Professor Dr. Hyuk-Jae Chang*; you have been a tremendous mentor to me. I would like to thank you for encouraging my research and for allowing me to grow as a research scientist. Your advice on both my research as well as my career have been priceless.

I would like to express the deepest appreciation to my committee chair *Professor Jung Sun Kim*; without his guidance and persistent help this dissertation would not have been possible. I would like to thank my committee members, *Professor Yang Soo Jang*, *Professor Jon Suh*, and *Professor Hae-Jeong Park*, whose work taught me that concern for cardiovascular disease evaluation should always transcend academic concerns and provide a quest for our times.

I would like to express my gratitude to *Professor Dr. Hackjoon Shim*, whose encouragements influenced my research. His role as my advisor

연세대학교
YONSEI UNIVERSITY

was essential to the pursuit of my vision. I also thank him for providing me learning opportunities through new experiences in addition to the research methods. I would like to thank *Professor Dr. Hyung-Bok Park*, who made time in her hectic schedule to provide me with valuable advice and offered unconditional support and mentorship throughout my Ph. D. course. I would like to thank *Professor Dr. Damini Dey*, who provided accurate guidance and constructive comments during my stay in the Biomedical Imaging Research Institute at the Cedars–Sinai Medical Center.

I sincerely acknowledge all my colleagues and dear friends. Their support sustained me as I worked to complete this study. I will remember all your contributions and hope to repay your kindness in the years to come. I would especially like to thank the physicians, specialists, and nurse aids in the Integrative Cardiovascular Imaging Research Center. All of you have been there to support me when I recruited subjects and collected data for my Ph.D. thesis. Finally, I would like to thank my beloved family. My father and mother's constant love and support have

연세대학교
YONSEI UNIVERSITY

helped me fulfill my dreams. Thank you once again. This thesis is dedicated to you all.

Youngtaek Hong

연세대학교
YONSEI UNIVERSITY

TABLE OF CONTENTS

연세대학교
YONSEI UNIVERSITY

연세대학교
YONSEI UNIVERSITY

LIST OF FIGURES

연세대학교
YONSEI UNIVERSITY

연세대학교
YONSEI UNIVERSITY

연세대학교
YONSEI UNIVERSITY

연세대학교
YONSEI UNIVERSITY

LIST OF TABLES

연세대학교
YONSEI UNIVERSITY

연세대학교
YONSEI UNIVERSITY

Abstract

Novel Methodology for Coronary Artery Disease Evaluation:
From a New Imaging Technique to Deep Learning Based Quantification

Youngtaek Hong

Department of Medical Science
The Graduate School, Yonsei University

(Directed by Professor Hyuk-Jae Chang)

Cardiovascular disease remains the leading cause of mortality in the world. Coronary computed tomographic angiography (CTA) has emerged as a reliable noninvasive modality for the diagnosis of coronary artery disease (CAD). However, on-site evaluation of CAD is still a challenging problem. To solve this problem, this dissertation covers methods ranging from a new imaging acquisition technique to deep learning based automatic quantification. To obtain quality CTA, catheter-directed selective CTA (S-CTA) was developed in the preclinical model, and the clinical feasibility of S-CTA was validated in patients who had diagnosed CAD. S-CTA successfully produced an optimal luminal enhancement with an extremely low-dose of iodine. Automatic quantification was developed using convolutional neural networks (CNN). We successfully measured vascular minimal lumen area, diameter stenosis, and plaque volume with the proposed CNN model. When S-CTA

연세대학교
YONSEI UNIVERSITY

was used for automatic quantification, the proposed CNN successfully captured intrinsic features of the contrast-enhanced lumen and calcified plaque better than C-CTA. S-CTA can be understood as an intraprocedural CTA modality under the combined-system that incorporates the coronary angiography system and a 320-detector row CT scanner. S-CTA enables a strategic stepwise approach for coronary catheterization and on-site evaluation for coronary stenosis.

Key words: cardiovascular disease, coronary angiography, multidetector computed tomography, machine learning, segmentation

연세대학교
YONSEI UNIVERSITY

Novel Methodology for Coronary Artery Disease Evaluation: From a New Imaging Technique to Deep Learning Based Quantification

Youngtaek Hong

Department of Medical Science
The Graduate School, Yonsei University

(Directed by Professor Hyuk-Jae Chang)

I. Introduction

1. Need for a new imaging technique

The coronary arteries supply blood into and out of the cardiac muscle, and they are mainly composed of the left and right coronary arteries. Coronary artery disease remains the leading cause of morbidity and mortality in the world. The multi-slice computed tomography scanners perform non-invasive imaging of the coronary artery. This approach, which is called coronary computed tomography angiography (CCTA), allows the visualization of the coronary lumen after intravenous injection of a contrast agent. CCTA has been established as the gold standard for the evaluation and treatment of coronary artery disease (CAD).[1, 2] However, it can only provide a 2-dimensional luminographic evaluation. There are several imaging acquisition modalities for coronary artery disease diagnosis such as intravascular ultrasound (IVUS)[3] and optical coherence tomography (OCT).[4] These invasive modalities have been adjunctively utilized for cross-sectional evaluation of the luminal

연세대학교
YONSEI UNIVERSITY

area, atherosclerotic plaque burden, and plaque characterization. This image information may be crucial for successful revascularization while minimizing the risk of complications.[5] Despite their efficacies, these modalities have several inherent limitations including high costs and high procedural risk based on their invasive nature.[6]

CCTA has grown into an attractive imaging modality for diagnosis of cardiovascular disease over the last decade. This is owing to technological advances such as an increase of detector rows and a reduction of gantry ration time of the computed tomography. These advantages allow non-invasive diagnosis of CAD and quantitative analysis of related clinical features such as luminal stenosis[7, 8] morphology and vulnerability of atherosclerotic plaque.[9, 10] In a quantitative comparative analysis of coronary artery lesions, it was found that minimal luminal area and area stenosis were not significantly different between CCTA and IVUS.[11] Unlike IVUS and OCT, CCTA is a three-dimensional image. Therefore, it can be utilized for morphological analysis and computational simulation such as hemodynamic analysis. In addition, this anatomical and physiological information can be used for procedural planning before coronary intervention. Despite these advantages, CCTA is not actively utilized during coronary artery catheterization. This is due to the lack of adequate access to the device, especially in cases where strategic stepwise approaches are needed for severe and complicated cases of CAD.[12]

연세대학교
YONSEI UNIVERSITY

2. Introduction of modality combined system

A recently introduced combined system, incorporating the coronary angiography system (INFX-8000C, Toshiba Medical Systems Corporation, Otawara, Japan) and a 320-detector row CT scanner (Aquilion ONE ViSION Edition), was shown to allow CTA scanning during coronary artery catheterization without the need to move the patient from the catheterization room to the CT room (Figure 1A, 1B). The purpose of this study is to develop a CCTA imaging protocol that can be applied to patients who are lying on the table for coronary artery intervention. Using the engaged guiding catheter for the intervention, the contrast medium can be directly injected into the target artery (Figure 1C). In this catheter-directed protocol, a coronary artery can be selectively imaged and then analyzed for quantitative measurement without further invasive manipulation such as IVUS or OCT. Therefore, this approach is expected to provide considerable and improved options for comprehensive CAD evaluation. Furthermore, it is expected that this technology will allow a significant reduction in the contrast dose required to perform comprehensive CAD evaluation. For a comprehensive evaluation of CCTA, accurate and elaborate quantification is a prerequisite. The importance of accurate quantification of atherosclerotic plaque in coronary arteries has been demonstrated by numerous invasive studies.[13, 14] The software required for CCTA analysis has recently been introduced to provide accurate assessment for plaque volume, plaque burden, and characterization in a semi- or fully automated manner.[15] However, these software require sophisticated manual adjustment to obtain a clinically meaningful measurement. Although a significant amount of research has been done on the

연세대학교
YONSEI UNIVERSITY

quantification of atherosclerotic plaques, their performance is still not suitable for clinical utilization. Recent research on setting the analysis parameters in the dedicated software for the CCTA is aimed toward obtaining clinically meaningful quantification results.[16]

연세대학교
YONSEI UNIVERSITY

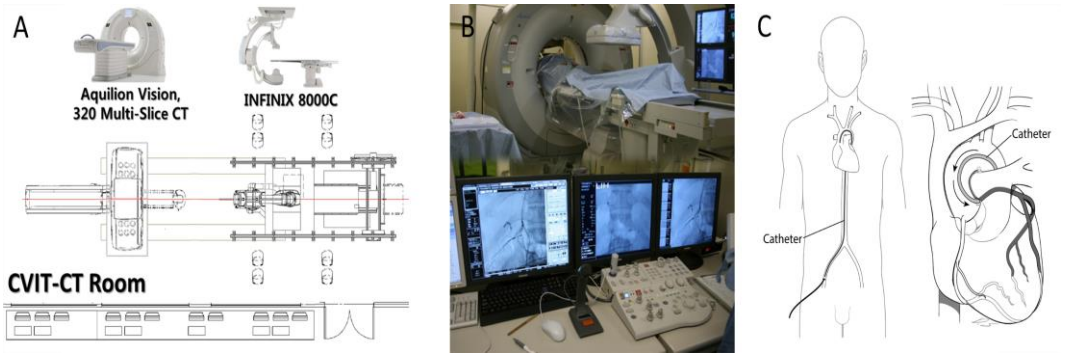

Figure 1 Schematic illustration (A) and actual image (B) of a novel cardiovascular interventional therapeutic CT system (CVIT-CT). This combined-modality approach, which incorporates the angiography system (INFX-8000C, Toshiba Medical Systems Corporation, Otawara, Japan) and a 320-detector row CT scanner (Aquilion ONE ViSION Edition) enables CT-scanning and angiography at the same site. (C) The diluted contrast medium can be selectively injected through the pre-engaged catheter during the CT scan.

연세대학교
YONSEI UNIVERSITY

3. Breakthrough in machine learning technique

Various machine learning techniques have recently made extensive progress in addressing computer vision problems such as classification and segmentation. Machine learning (ML)—a discipline that enables computers to learn without being programmed through developed algorithms derived from data—has been applied for automated disease diagnosis.[17-19] ML can be performed by a myriad of methods and is ubiquitous in the fields of internet search, financial analyses, and fraud detection. In ML, a convolutional neural network (CNN) is a type of neural network that features huge improvements not only in whole-image classification but also in object detection.[20-22] CNNs are also driving advances in medical image processing.[23, 24] They showed the utility and efficacy of a CNN architecture for semantic segmentation such as the labeling problem in medical imaging. In this study, a CNN based plaque quantification method that can produce clinically relevant results is proposed.

연세대학교
YONSEI UNIVERSITY

II. **Feasibility of Selective Catheter-Directed Coronary Computed Tomography Angiography Using Ultralow-Dose Intracoronary Contrast Injection in a Swine Model**

1. Material and Methods

A. Animal preparation

The Institutional Animal Care and Use Committee (IACUC, Yonsei University Health System at Seoul) approved this study protocol. Female swine (n=4, approximately 35–40kg) were acclimated in our animal facility (Department of Laboratory Animal Medicine, Medical Research Center, Yonsei University College of Medicine) for 7–10 days before the CT examination was performed. On the day of the examination, each animal was medicated with an intramuscular mixture of enrofloxacin (5mg/kg) and atropine (0.05mg/kg) prior to any procedure. Sedation was induced by a combination of tiletamine (Zoletil 50, Virbac) 5mg/kg and xylazine (Rompun, Bayer). Intravenous (IV) access was obtained via an ear vein with a 20-gauge catheter. The sedated animal was transported from the animal facility to angiography and CT combined-system for catheterization. Once placed on the device table, a mechanical ventilator maintained sedation with the oxygen level set at 1–2L/min. A mixture of 2% isoflurane (Forane) and 4 mg vecuronium bromide (0.10mg/kg) was infused intravenously to obtain muscle relaxation. The right carotid artery was cut down with a guiding sheath to advance the catheter into the coronary artery. A guiding catheter (Cordis, JL 5-3.5) was engaged through the inserted sheath and selectively engaged in the right coronary artery (RCA) or left anterior descending (LAD) branch to perform the selective

연세대학교
YONSEI UNIVERSITY

CCTA study. Conventional coronary angiography was performed by manual injection of 5 mL of contrast medium (320 mgI/mL iodixanol; Visipaque; GE Healthcare, Princeton, NJ) to confirm the appropriate catheter engagement in order to perform the angiogram. The heart rate was controlled with IV bolus of 40mg of esmolol to acquire a target heart rate range of 70-80 beats per minute from the initial range of 100-120 beats per minute.

연세대학교
YONSEI UNIVERSITY

B. CT protocols

A 320-multidetector CT scanner (Aquilion ONE; Toshiba Medical Systems Corporation, Otawara, Japan) was employed to perform the CT scan. The ventilator was briefly stopped to achieve breath hold during CT scanning. The CT scan was performed using a cranial-to-caudal acquisition with retrospective ECG-gating using the following parameters: collimation and slice thickness, 0.5mm; reconstruction increment, 0.3 mm; tube rotation time, 0.35 s; tube voltage, 120kVp; current, 550mA; and reconstruction field of view, 109–123mm. The data were reconstructed at 75% of the R-R length for all studies. If motion artifacts were present, a different cardiac phase was selected. The following modulation was applied to the reconstruction: kernel, FC43; reconstruction algorithm, adaptive iterative dose reduction (AIDR) 3D.

연세대학교
YONSEI UNIVERSITY

C. Selective CCTA study

The contrast medium (Iomeron 400 mg/mL; Bracco, Milan, Italy) was diluted with normal saline to obtain optimal coronary enhancement (250–350 HU).[25, 26] Contrast medium was adjusted to a concentration of 13.13mgI/mL in order to obtain 350HU with 120kVp of CT voltage. The diluted contrast medium was delivered with a dual-head power injector (Medrad Stellant Injector; Medrad, Indianola, PA) using the following protocols: protocol 1 (P1), injection rate and volume of contrast medium, 2 mL/s, 20 mL; protocol 2 (P2), 3 mL/s, 20 mL; protocol 3 (P3), 3 mL/s, 30mL; protocol 4 (P4), 4 mL/s, 20 mL; and protocol 5 (P5), 4 mL/s, 30mL. These parameters are summarized in Table 1. A selective CCTA scan was simultaneously performed with injection of the contrast medium. A retrospective ECG-gating was used without dose modulation. The scanning duration was fixed to 10s in order to blind the examiner to the injection rate and volumes for each of the examined protocols. Therefore, actual injection times were different from protocol to protocol (Figure 2). We acquired continuous volumes (average 6-7 sets of volumes) over the 10s scan duration. The interval between injections was 5 min, to allow elimination of contrast medium from the coronary artery and to ensure the animal condition was clinically stable. These protocols were separately performed in each LAD and RCA artery; thus, we could selectively obtain CT images of each of the coronary arteries individually.

연세대학교
YONSEI UNIVERSITY

Table 1 Protocols for Selective CCTA studies

Protocol	Voltage (kVp)	Current (mA)	Concentration of CM (mgI/mL)	Volume (mL)	Injection Rate (mL/s)	Iodine Flux (mgI/s)
P1	120	550	13.13	20	2	26.26
P2	120	550	13.13	20	3	39.39
P3	120	550	13.13	30	3	39.39
P4	120	550	13.13	20	4	52.52
P5	120	550	13.13	30	4	52.52

CM = Contrast medium

연세대학교
YONSEI UNIVERSITY

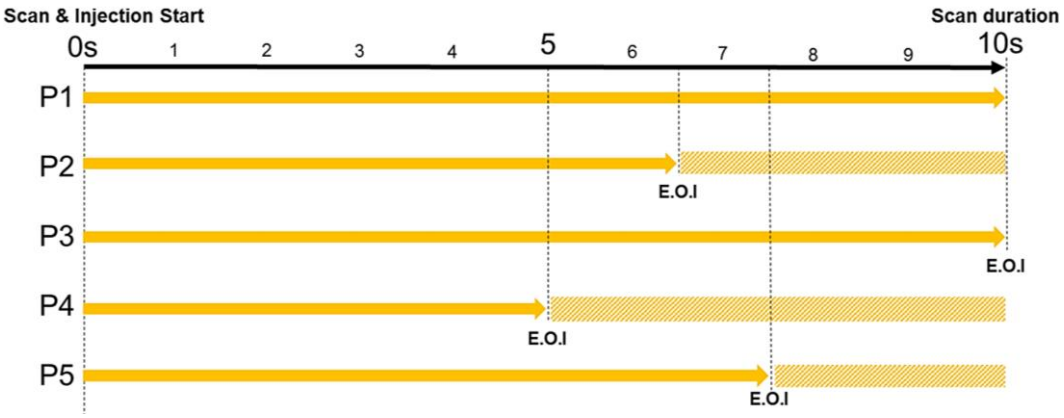

Figure 2 The selective CCTA scan was simultaneously performed with the contrast injection. But the examined protocols (P1 – P5) have different injection duration. E.O.I - end of injection.

연세대학교
YONSEI UNIVERSITY

D. IV CCTA study

The protocol for the IV CCTA study (P_{IV}) was performed with 60mL contrast medium at 5mL/s flow rate, and 30mL of saline flush at the same flow rate using a dual-head power injector. The timing-bolus technique was utilized by monitoring the contrast values in the ascending aorta. Serial monitoring for bolus tracking was simultaneously initiated with low-dose (120 kV, 20 mAs) contrast medium injections. When the values in the ascending aorta reached 180HU, the CT scan was started automatically with retrospective ECG-gating.

연세대학교
YONSEI UNIVERSITY

E. Image Analysis

Selective CCTA images were transferred to a workstation (Vitrea fx6.4, Vital Images). A level III CT reader who was blinded to the selective CCTA protocols chose representative images for each of the protocols and selected the best phase to minimize motion artifacts as well as enhance the distal part of the arteries using 3D rendered images and maximum intensity projection images, when necessary. Representative images were transferred via portable USB drive to another standalone workstation (QAngio CT workstation, version 2.0.2; Medis Medical Imaging Systems, Leiden, Netherlands) to delineate the luminal boundary and analyze luminal intensities.

Measurements were made in the proximal, mid, and distal segments of the RCA and LAD, according to the Society of Cardiovascular Computed Tomography's anatomy definitions.[27] The cross-sectional intensities were automatically recorded with 0.5-mm intervals. A transluminal attenuation gradient (TAG), defined as the linear regression coefficient between the luminal CT value and the length of the centerline of the measured coronary artery, was used.[28] A representative example of TAG measurement is displayed in Figure 3.

연세대학교
YONSEI UNIVERSITY

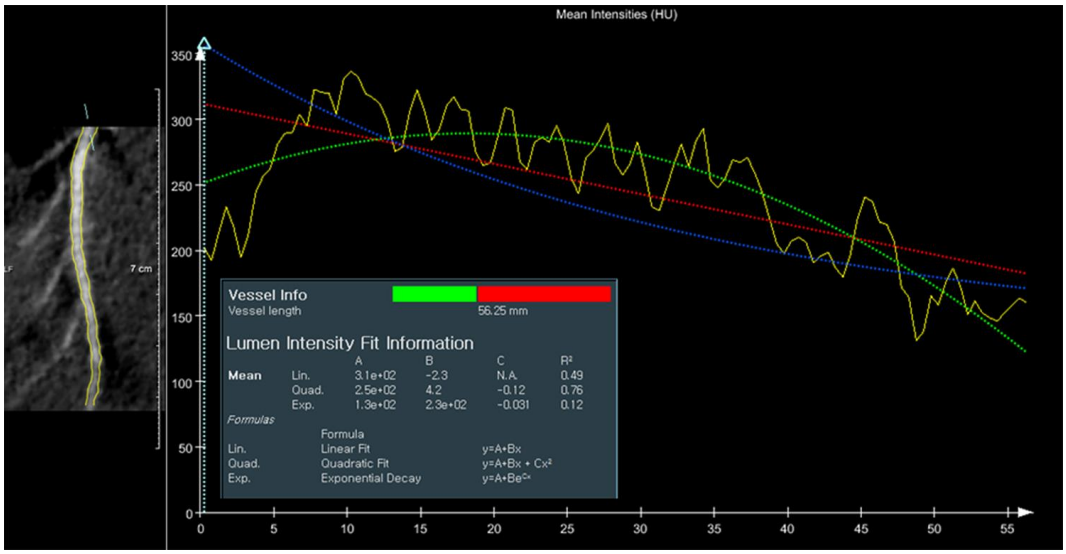

Figure 3 Representative transluminal attenuation gradient (TAG) measurement images with the Q Angio-CT device. The TAG value was calculated automatically after the luminal attenuation measurement in the Q Angio-CT. The gradient of the linear fit formula for lumen intensity information indicates the TAG value for the image that was scanned with a representative selective coronary computed tomography angiography protocol (P1).

연세대학교
YONSEI UNIVERSITY

F. Statistical Methods

A mixed model, involving the least squared means with Bonferroni correction was employed to evaluate the statistical significance of attenuation values between both studies. Attenuation values were expressed as means and standard error (SE). The 95% confidence interval was used to report associations in accordance with an optimal enhancement range of 250–350 HU. Differences in the least squared means were used to compare mean values among the protocols with partial segments. All statistical analyses were performed using SAS statistical software (SAS System for Windows; Version 9.2, SAS Institute, Cary, NC, USA).

연세대학교
YONSEI UNIVERSITY

2. Results

The mean attenuation and SE values of the selective CCTA (P1, P2, P3, P4, and P5) and IV CCTA (P_{IV}) studies are summarized in Table 2. In the per-vessel analysis, the mean attenuation value of all selective CCTA protocols was within the range of 250–350 HU, which is generally considered the optimal range. In the per-segment analysis, the mean attenuation values of the selective CCTA studies were in accordance with the suggested optimal contrast enhancement range for the proximal and middle segments. However, the attenuation values for the distal LAD in all selective CCTA protocols (P1~P5) and for the distal RCA in P2 were <250HU. The attenuation values of selective CCTA were generally higher for the RCA than for the LAD. The IV CCTA was over-enhanced, and the attenuation value was >350HU in this study. We performed IV CCTA using 1.5mL/kg of contrast medium, as performed in a previous study.[29] All selective CCTA protocols used in the current study were adequate for clinical use as the respective mean attenuation values were within the optimal range. The P1 was considered the best protocol because the 95% confidence intervals of the attenuation range best fit within the optimal contrast enhancement range (mid LAD, mid-RCA, distal RCA). In contrast, the P3 only demonstrated optimal enhancement range for the proximal RCA, while P2 and P4 showed optimal enhancement for the proximal and mid-RCA, and the P5 protocol for the distal RCA only.

However, the 95% confidence intervals of the IV CCTA studies exceeded the optimal enhancement range (Figure 4). In view of the 95% confidence intervals, the P1 was regarded to be the best representative protocol of selective CCTA studies. Representative images of

연세대학교
YONSEI UNIVERSITY

P1 are further displayed in Figure 5. The TAG values of P1 and P_{IV} were compared to determine any differences in attenuation homogeneity, with values closer to zero implying greater homogeneity. In Figure 6, we observed that the TAG of P1 was more homogeneous than P_{IV} (LAD: -1.5245 vs. -1.7558, $p<0.001$; RCA: 0.0459 vs. 0.0799, $p<0.001$).

연세대학교
YONSEI UNIVERSITY

Table 22 Luminal attenuation values and heart rates for the examined protocols

	P1	P2	P3	P4	P5	P_{IV}
Per vessel						
LAD	270.3 ± 20.4	262.9 ± 20.4	276.8 ± 20.4	268.0 ± 20.4	251.3 ± 20.4	389.9 ± 20.5
RCA	322.6 ± 7.4	264.7 ± 7.4	274.0 ± 7.4	277.7 ± 7.4	334.7 ± 7.4	354.4 ± 7.7
Per segment						
pLAD	284.2 ± 23.1	294.7 ± 23.1	300.4 ± 23.1	287.2 ± 23.1	294.6 ± 23.1	425.9 ± 23.2
mLAD	297.6 ± 19.9	277.5 ± 19.9	277.4 ± 19.9	284.7 ± 19.9	250.2 ± 19.9	413.4 ± 18.5
dLAD	230.0 ± 18.4	216.4 ± 18.4	240.5 ± 18.5	232.8 ± 18.4	205.1 ± 18.4	335.6 ± 18.5
pRCA	341.6 ± 8.0	282.7 ± 8.0	294.2 ± 8.0	289.1 ± 8.0	351.0 ± 8.0	357.4 ± 8.8
mRCA	319.3 ± 7.4	275.1 ± 7.4	265.6 ± 7.5	291.2 ± 7.4	352.5 ± 7.4	361.8 ± 8.0
dRCA	302.4 ± 16.7	230.8 ± 16.7	253.3 ± 16.8	254.4 ± 16.7	296.8 ± 16.7	349.2 ± 16.8
HR (beats/min)	64 ± 2	66 ± 3	65 ± 4	66 ± 4	65 ± 1	64 ± 3

Attenuation values are given as mean ± SE (standard error).

LAD – left anterior descending artery; RCA – right coronary artery; p, m, d – proximal, middle, distal. HR – Heart rate during scanning (beats/min) was given as mean ± SD (standard deviation).

연세대학교
YONSEI UNIVERSITY

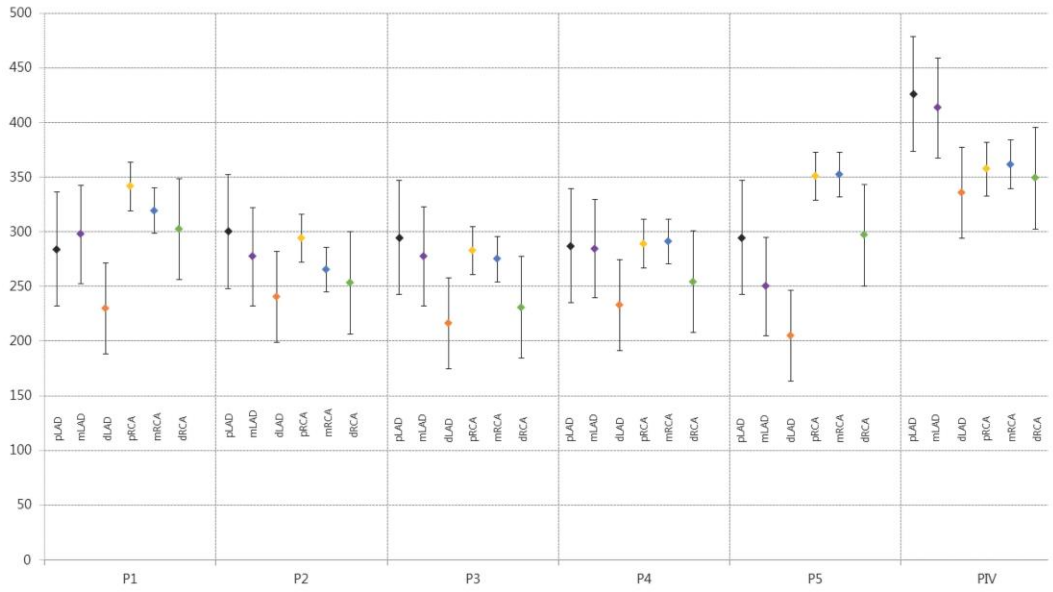

Figure 4 Confidence interval of luminal attenuation values. The confidence interval indicates the enhancement of the selective coronary computed tomography angiography (CCTA) study. The representative selective CCTA protocol (P1) was in accordance with the optimal enhancement range (250–350HU) in the mid LAD, mid-RCA, and distal RCA. Black is proximal LAD; purple is mid LAD; orange is distal LAD; yellow is proximal LAD; blue is mid LAD and green is distal LAD.

연세대학교
YONSEI UNIVERSITY

3. Discussion

The current study is, to our knowledge, the first to document the feasibility of catheter-directed selective CCTA using a combined modality system. In this study, we could establish a useful protocol for selective CCTA. We could successfully obtain optimal contrast enhancement in the range of 250–350 HU by using an ultra-low-dose concentration of 13.13mgI/mL. Further, the entire selective CCTA protocol revealed stable contrast enhancement compared with conventional IV CCTA at a clinically usable level. The iodinated contrast medium has been shown to have a dose-dependent relationship with contrast-induced nephropathy (CIN)[30] and implying the need for minimizing the contrast dose to prevent CIN.[31] In the current study, we could significantly reduce the amount of iodine by using ultra-low-dose contrast medium necessary for selective CCTA.

This direct injection of diluted iodine contrast has previously been tested in post-mortem studies and demonstrated the ability to clearly visualize the coronary trees and plaques.[32] The representative protocol (P1) contains the 263 mg of iodine to produce the optimal enhancement range, which was 1.09% of the amount for the conventional method (P_{IV}). Therefore, we suggest that this extremely small amount of contrast may be adequate for optimal imaging while possibly reducing the risk of CIN in patients undergoing PCI.

연세대학교
YONSEI UNIVERSITY

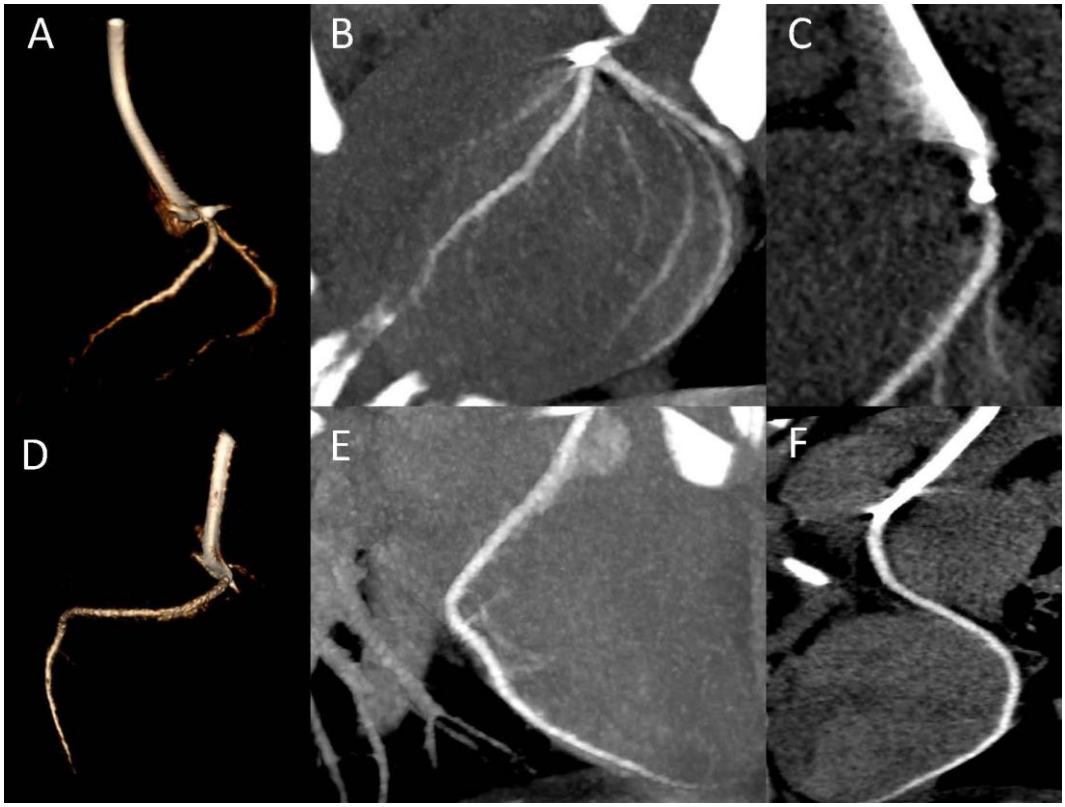

Figure 5 Representative images of the left anterior descending (LAD) and right coronary (RCA) arteries using P1 from the selective coronary computed tomography angiography (CCTA) protocols. A: 3D rendered image of LAD; B: maximum intensity projection image of LAD; C: curved multi-planar reconstruction images of LAD; D: 3D-rendered image of RCA; E: maximum intensity projection image of RCA; F: curved multi-planar reconstruction images of LAD. These images indicate that P1 yielded adequate luminal at-

연세대학교
YONSEI UNIVERSITY

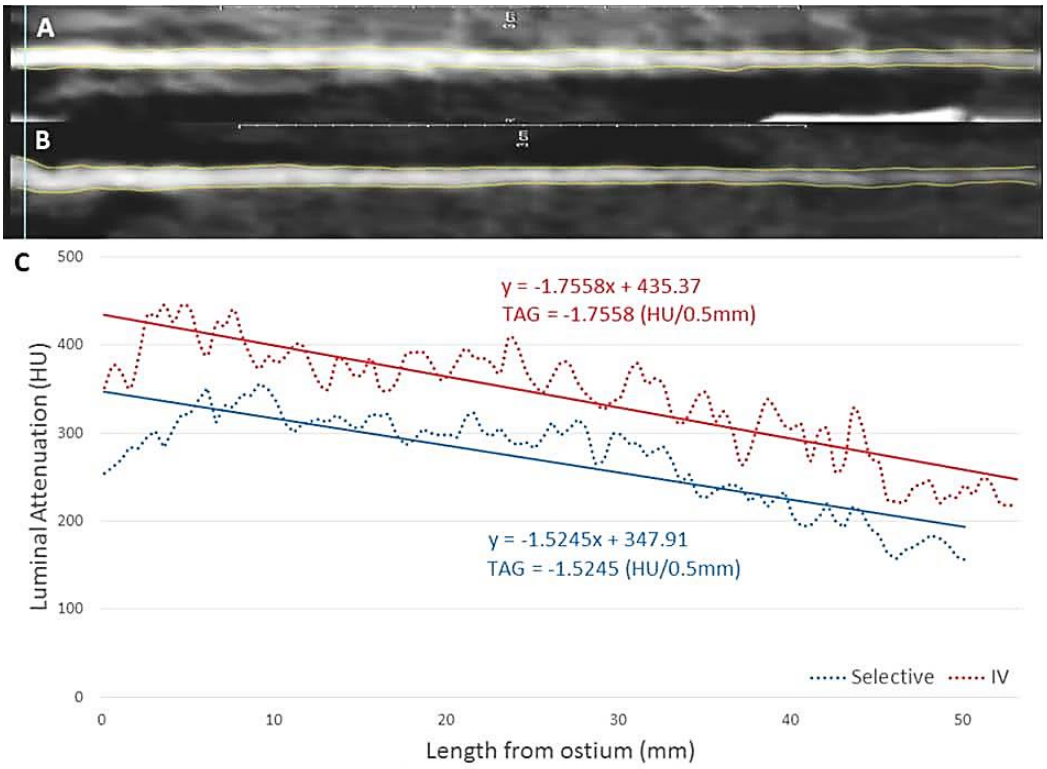

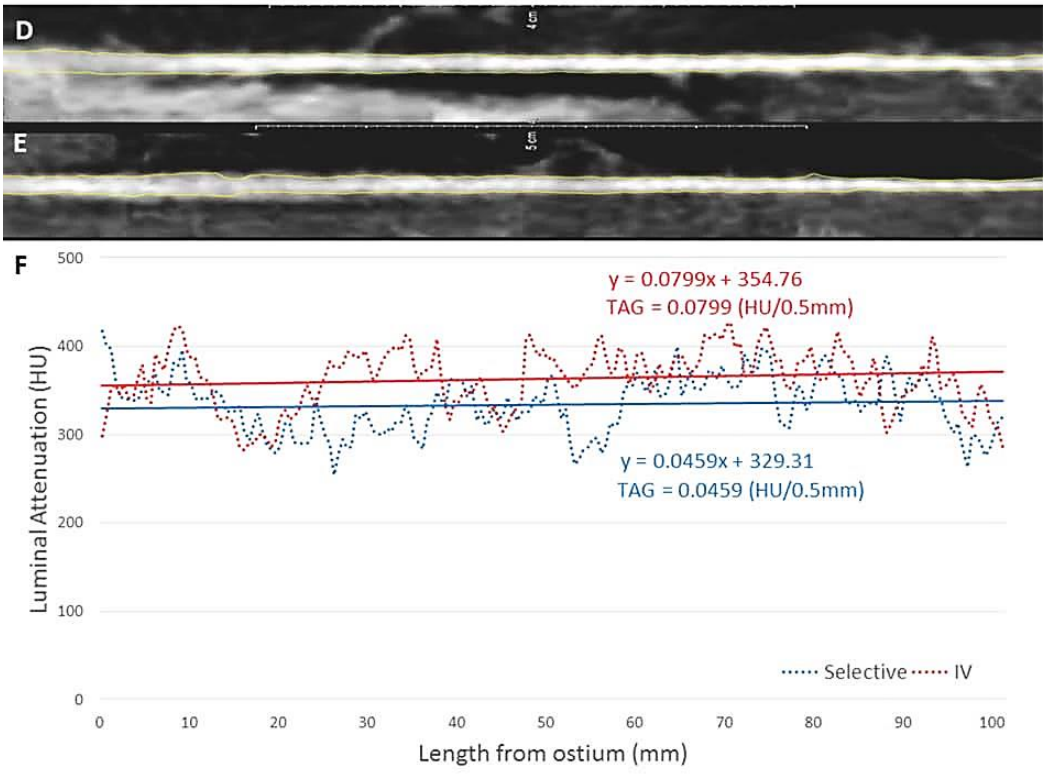

연세대학교
YONSEI UNIVERSITY

Figure 6. Comparison of transluminal attenuation gradient (TAG) for the representative case P1 and PIV in the left anterior descending (LAD) and right coronary (RCA) arteries. A:stretched view of the LAD with PIV of the IV study; B:stretched view of the LAD with P1 of the selective coronary computed tomography angiography (CCTA) study; C: TAG for the LAD was compared between the PIV and the representative case P1 (-1.5245, -1.7558, respectively); D:stretched view of the RCA with PIV of the IV study; E:stretched view of the RCA with P1 of the selective CCTA study; F: TAG for the RCA was compared between the PIV and the representative case P1 (0.0459, 0.0799, respectively).

연세대학교
YONSEI UNIVERSITY

Few prior studies have attempted to lower the amount of contrast medium using catheter-based CCTA. A previous study using superior vena cava (SVC) catheter-directed CCTA was able to depict the coronary anatomy with adequate attenuation (HU > 250) using 50 mL of contrast material.[33] In that study, the pooled attenuation was similar to conventional IV CCTA using 100 mL of contrast medium, which showed only 50% reduction of contrast medium. Another study using aortic-root catheter-directed enhancement also reduced the amount of contrast medium to as little as 20mL.[29] However, that study required a specialized multi-hole pigtail catheter and still showed only 80% reduction of contrast medium. On the other hand, our technique uses a conventional coronary angiography catheter, which is commonly used during coronary catheterization for injecting contrast medium at an extremely low contrast dose (99% reduction). Moreover, the previously mentioned studies displayed an extremely high enhancement rate in proximal coronary artery segments with a rapid decreasing pattern of enhancement in distal regions, whereas our study found all segments of the coronary arteries examined to be relatively homogeneous. Previous studies used full- or half-concentrated contrast medium and introduced it into the SVC or aortic root, which made it difficult to control attenuation in the coronary arteries. However, the unique design of our study permitted us to modulate the concentration of contrast medium to obtain targeted enhancement. In addition, previous techniques had to inherently consider many patient-dependent factors such as body mass index, pulmonary circulation system, and aortic valve pathology; whereas our selective CCTA technique was independent of these factors, with the exception of the need for catheter engagement. The advent of the 320-detector row CT scan has allowed imaging of the entire coronary artery

연세대학교
YONSEI UNIVERSITY

tree during a single cardiac cycle. A TAG has been shown to be a useful tool for the evaluation of coronary artery stenosis[28] and also for assessing the physiological significance of stenosis.[34] Foremost, the current study demonstrated the feasibility and clinical utility of selective CCTA utilizing TAG values as compared with IV CCTA.

This study is not without limitations. In order to obtain the peak enhancement timing for the CT scan as well as the optimal contrast injection duration, we had to perform a retrospective ECG-gating CT scan over 10s to cover the entire injection duration, which inevitably caused the elevation of radiation dose. Furthermore, we used a tube voltage of 120kVp, which further increased the radiation hazard. Although less contrast injection time (<5 s) has been recommended to reduce the cardiac ischemic burden[35], we used a relatively longer injection time (~10 s) to search for an optimal contrast injection duration and to avoid analytical bias, which may increase myocardial ischemia. In addition, the diagnostic catheter tip engaged the ostium of the coronary arteries, often making evaluation of the left main or ostial portion of RCA difficult. The attenuation value at the catheter-tip is >1000 HU because of the material's composition. Thus a beam-hardening artifact is created around the tip. Another limitation of this study is that the LCx was not included in the analysis. When we tried to engage the left coronary artery system with the guide catheter, it frequently engaged the LAD selectively, and due to the high anatomical variances in the LCx between porcine models, the catheter was intentionally fixed to engage and primarily visualize the LAD. Finally, similar to conventional angiography catheter-related complications, our novel technique may be prone to complications including coronary artery dissection, spasm, stroke, and even death during selective CCTA; albeit, the complication rates

연세대학교
YONSEI UNIVERSITY

are in general, extremely low.[36] Forthcoming studies involving humans are warranted to further establish the optimal protocol[37] and to confirm the feasibility of this technique.

In conclusion, the catheter-directed selective CCTA can produce an optimal contrast enhancement with ultra-low-dose contrast medium. This technique may provide additional means of coronary evaluation in patients who may require strategic planning prior to procedure utilizing a combined modality system.

연세대학교
YONSEI UNIVERSITY

III. Clinical Feasibility of Selective Catheter-Directed Intracoronary Computed Tomography Angiography Using Extremely Low-Dose of Iodine in Patients with Coronary Artery Disease

1. Material and Methods

A. Study population

We prospectively included 65 consecutive patients who underwent C-CTA and were scheduled to undergo ICA for clinical indications. Patients with body weight <85 kg, heart rate <65 beats per minute during CT scan, and diameter stenosis of 25–99% at the left anterior descending, left circumflex, or right coronary artery were included. In patients with multivessel disease, only one vessel with severe stenosis was included. In contrast, pregnant patients and those with prior coronary artery bypass grafting surgery, contraindications to iodinated contrast material, hemodynamic instability, renal insufficiency (serum creatinine level >1.5 mg/dL or 133 μmol/L), absent sinus rhythm, and inability to hold their breath were excluded. The institutional review board of Yonsei University College of Medicine, Seoul, Korea, approved the study protocol, and all patients provided written informed consent.

연세대학교
YONSEI UNIVERSITY

B. C-CTA protocol

Before CT scanning, all patients received a 0.3-mg sublingual dose of nitroglycerin. If their heart rate was higher than 65 beats per minute, patients also received a single oral dose of 50 mg metoprolol tartrate (Betaloc, Yuhan) unless beta-adrenergic blocking agents were contraindicated. C-CTA was performed on 320-slice CT scanner (Aquilion ONE ViSION Edition, Toshiba). Bolus tracking was used by placing the region of interest (ROI) in the ascending aorta, and scanning was started at 2 s after reaching the predefined threshold of 180 Hounsfield units (HU). A 60–90 mL of contrast medium (370 mg iodine/mL, Iopamiro, Bracco) was used at a flow rate of 5 mL/s using a dual-head power injector (Medrad Stellant injector, Medrad) via the antecubital vein. Prospective electrocardiographic (ECG) gating with the following scan parameters was used: rotation time, 350 ms; tube voltage, 100–120 kVp; tube current, 600–800 mA; and slice collimation, 320 × 0.5 mm. CTA images were reconstructed using a slice thickness of 0.5 mm at 75% of R-R interval, and FC04 as the convolution kernel and adaptive iterative dose reduction 3D as the reconstruction technique were used. Dose length product (mGy × cm) was recorded and then presented as mSv (mGy × cm × 0.014).

연세대학교
YONSEI UNIVERSITY

C. S-CTA protocol

Following the developed protocol in swine model [38], S-CTA was performed using 13.13 mg iodine/mL of diluted contrast material at an injection rate of 2 mL/s with tube voltage of 120 kV and current of 550 mA. In this study, the protocol was optimized according to clinical application: 17.19 mg iodine/mL at an injection rate of 5 mL/s with tube voltage of 100 kV in patients with a body mass index <30 kg/m^2 and 120 kV otherwise. The contrast medium was delivered via a 5-French Judkins diagnostic catheter (left or right) using a dual-head power injector (Medrad Stellant injector, Medrad). S-CTA was started at 1 s after the injection of contrast material to allow the contrast material to fully fill the target vessel. Prospective ECG gating was used in the same manner as in C-CTA; the same scan parameters in C-CTA were applied in S-CTA. The scan parameters are compared in Table 3.

연세대학교
YONSEI UNIVERSITY

D. Luminal enhancement analysis

S-CTA and C-CTA images were transferred to a standalone workstation (QAngio CT workstation, version 2.0.5; Medis Medical Imaging Systems, Leiden, Netherlands) to evaluate luminal enhancement and to delineate wall boundary. An experienced level III CT reader manually evaluated luminal enhancement in HU at the proximal, mid, and distal segments of each vessel such as left anterior descending (LAD), left circumflex artery (LCx), and right coronary artery (RCA) according to the Society of Cardiovascular Computed Tomography's anatomy definitions[27] with cross-sectional intensities automatically recorded at 0.5 mm intervals. Transluminal attenuation gradient (TAG)[28], determined from the change in HU per 10-mm length of coronary artery and defined as the linear regression coefficient between the luminal HU and length of the evaluated vessel from the ostium (millimeters), was used for assessing the luminal homogeneity of artery (Table 4).

연세대학교
YONSEI UNIVERSITY

Table 3. Protocol summary for S-CTA and C-CTA

	Protocol for S-CTA	Protocol for C-CTA
CT scanner	320-slice CT scanner (Aquilion ONE ViSION Edition)	320-slice CT scanner (Aquilion ONE ViSION Edition)
ECG gating	Prospective	Prospective
Rotation time	350 ms	350 ms
Slice collimation	320 × 0.5 mm	320 × 0.5 mm
Tube voltage	100–120 kVp	100–120 kVp
Tube current	600–800 mA	600–800 mA
Slice thickness	0.5 mm	0.5 mm
Iodine injection		
Technique	By engaged catheter	By intravenous infusion
Rate	5 mL/s	5 mL/s
Volume	15 mL	60–90 mL/s
Concentration	17.19 mg iodine/mL	370 mg iodine/mL
Radiation dose	2.71 ± 1.10 mSv	3.52 ± 2.50 mSv

The effective radiation dose was significantly different ($p < 0.0001$). S-CTA, selective computed tomography angiography; C-CTA, conventional computed tomography angiography; CT, computed tomography; ECG, electrocardiographic.

연세대학교
YONSEI UNIVERSITY

E. CTA analysis

C-CTA and S-CTA were analyzed on a standalone workstation with dedicated software (QAngio CT version 2.0.5, Medis Medical Imaging Systems) by an expert reader with level III certification in cardiac CT. The analysis was performed using a standard 17-segment model [27] up to a luminal diameter limit ≥1.5 mm. To evaluate luminal enhancement, mean and standard deviation (SD) were calculated for per-vessel and per-segment analyses. Transluminal attenuation gradient (TAG) [28], defined as the linear regression coefficient for luminal enhancement changes along the artery axis, was calculated to evaluate homogeneity of luminal enhancement. Image noise, signal-to-noise ratio (SNR), and contrast-to-noise ratio (CNR) were measured. The reader placed the ROI in the proximal artery (ROI_1) and in the adjacent non-enhanced pericardial fat tissue (ROI_2) at matched location on S-CTA and C-CTA (Figure 7). Image noise was defined as an SD of ROI_1; SNR was calculated by dividing the average HU of ROI_1 by image noise. CNR was calculated using the following formula: CNR = (average HU of ROI_1 − average HU of ROI_2)/image noise.

연세대학교
YONSEI UNIVERSITY

Table 4 Luminal enhancement and TAG on S-CTA and C-CTA

	Vessel (n = 110)	Proximal (n = 110)	Middle (n = 110)	Distal (n = 110)
Luminal enhancement (mean ± SE)				
S-CTA	324.4 ± 8.0 HU	344.6 ± 8.1 HU	334.0 ± 8.8 HU	298.1 ± 8.9 HU
C-CTA	312.0 ± 8.0 HU	357.9 ± 8.1 HU	312.9 ± 8.8 HU	270.5 ± 8.9 HU
p value	<0.0001	<0.0001	<0.0001	<0.0001
TAG				
S-CTA	-0.65	-0.20	-0.28	-1.03

Transluminal attenuation gradient (TAG) values at distal segment were not the statistically significant difference (p =0.002), however, other measurements significantly different between S-CTA and C-CTA (p <0.0001). HU = Hounsfield Unit, SE = standard error.

연세대학교
YONSEI UNIVERSITY

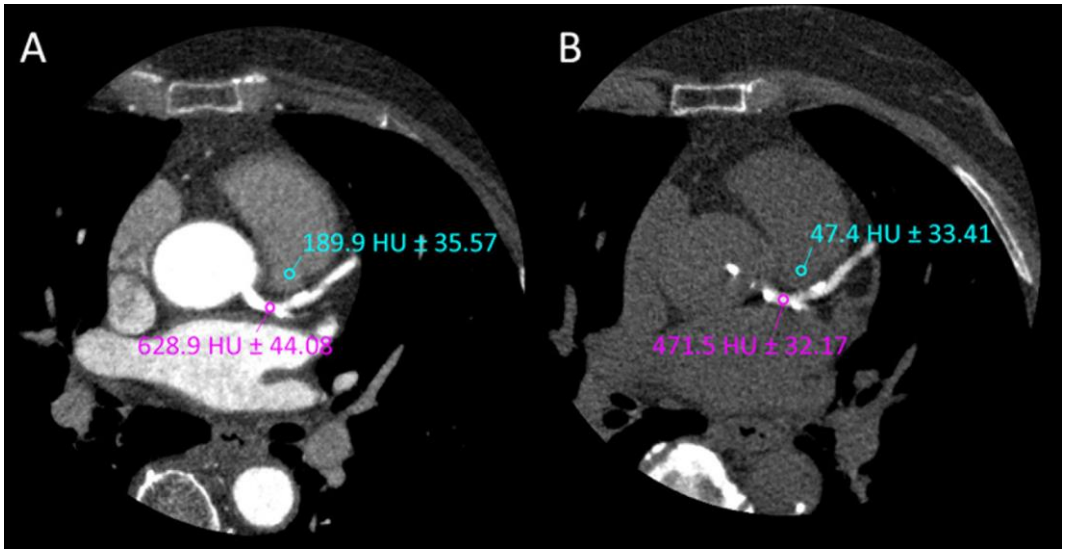

Figure 7 The region of interest (ROI) placement at a matched location between S-CTA and C-CTA. (A) ROI placement of C-CTA was shown with magenta and cyan color. (B) ROI placement of S-CTA was shown at the matched location with S-CTA. In these example images, C-CTA shows that image noise: 44.08 HU, SNR: 14.27, and CNR: 9.96 and S-CTA shows show that image noise: 32.17 HU, SNR: 14.66, and CNR: 13.18.

연세대학교
YONSEI UNIVERSITY

F. Plaque volume analysis

Plaque was semi-automatically measured, and revisions to our previously described method were made [39, 40]. An example of plaque lesion assessment is shown in Figure 8. Plaque volume (PV) and percent aggregate plaque volume (%APV) were measured in 44 lesions. PV was calculated as vessel volume minus lumen volume in each lesion segment. %APV was calculated by dividing APV by total vessel volume, and APV was defined as the total PV in each artery.

연세대학교
YONSEI UNIVERSITY

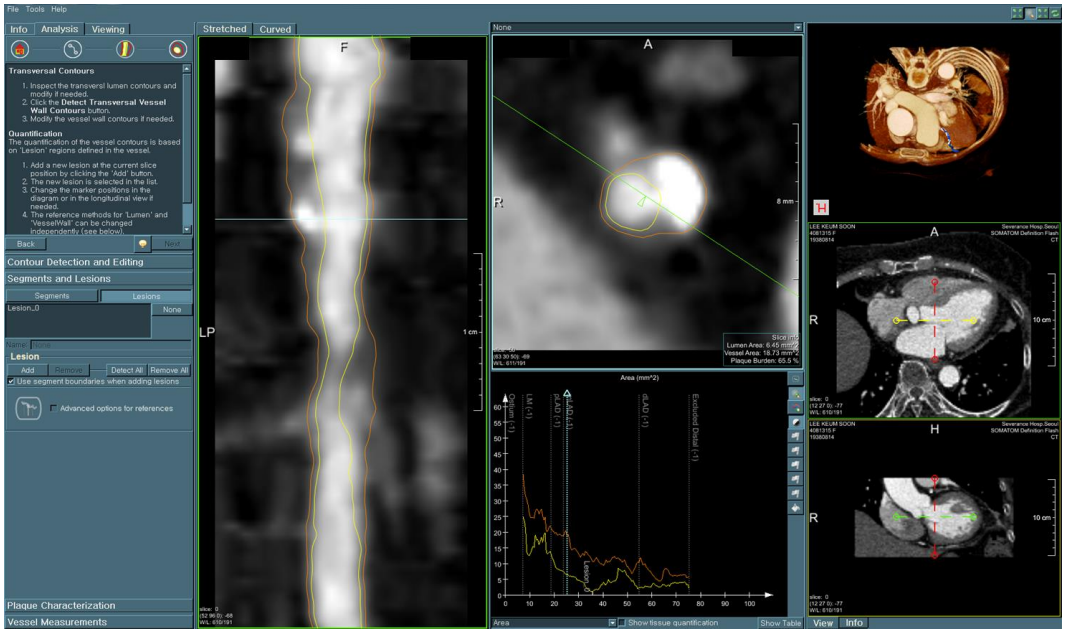

Figure 8 Representative plaque volume measurement. The expert manually edited the inner lumen and outer vessel wall contours.

연세대학교
YONSEI UNIVERSITY

G. Statistical Analysis

Continuous variables are expressed as means ± SD if normally distributed or median (interquartile range) if non-normally distributed. Paired Student's *t*-test and Pearson's correlation coefficient using two-sided p values were employed to compare S-CTA and C-CTA, with Fisher's z-transformation statistic used to compare correlations. A mixed model reporting the differences in the least square means with Bonferroni post hoc correction was employed to assess the statistical significance of luminal enhancement values expressed as mean ± standard error in the comparison between S-CTA and C-CTA. Bland–Altman plots with 95% confidence intervals were also constructed to display the correlations between S-CTA and C-CTA. Statistical analysis was performed using SAS version 9.2 (SAS Institute) and MedCalc version 12.7.5 (MedCalc Software bvba). A p value of less than 0.0001 was considered statistically significant.

연세대학교
YONSEI UNIVERSITY

2. Results

A. Clinical characteristics.

Patient characteristics are presented in Table 5. The study cohort included 39 males (60%), and the mean age was 64.3 ± 10.2 years. Body mass index and risk factors for CAD at the time of CTA examination are listed in Table 5. The mean time difference between S-CTA and C-CTA was 5.8 days. No specific complications occurred after any of S-CTA and coronary artery interventions.

연세대학교
YONSEI UNIVERSITY

Table 5 Patient Characteristics

Patient characteristics	n = 65
Age, years (mean ± SD)	64.3 ± 10.2
Male, n (%)	39 (60)
Weight, kg (mean ± SD)	66.2 ± 9.9
Body mass index, kg/m2 (mean ± SD)	24.7 ± 2.8
Risk factors	
Hypertension, n (%)	27 (42)
Hyperlipidemia, n (%)	42 (65)
Diabetes mellitus, n (%)	46 (71)
Current smoker, n (%)	23 (35)
Distribution of examined vessel	
Left anterior descending artery, n (%)	55 (46)
Left circumflex artery, n (%)	55 (46)

Values are mean ± standard deviation, or n (%).

연세대학교
YONSEI UNIVERSITY

B. Luminal enhancement analysis

In the per-vessel analysis, luminal enhancement was significantly higher on S-CTA than on C-CTA (324.4 ± 8.0 HU vs. 312.0 ± 8.0 HU, $p < 0.0001$). In the per-segment analysis, luminal enhancement was higher in the proximal segment only on C-CTA than on S-CTA; however, luminal enhancement was higher in the middle and distal segments on S-CTA than on C-CTA. All luminal enhancement ranges were significantly different between S-CTA and C-CTA ($p < 0.0001$). Figure 9 shows a representative case example of S-CTA and C-CTA images obtained from the same patient in our study. TAG was compared in the per-vessel and per-segment analyses. In the per-vessel analysis, TAG showed a significantly slower reduction pattern on S-CTA than on C-CTA (-0.65 HU/10 mm vs. -0.89 HU/10 mm, $p < 0.0001$). In the per-segment analysis, TAG on S-CTA showed a more than twofold slower reduction pattern than that on C-CTA in the proximal segment (-0.20 HU/10 mm vs. -0.65 HU/10 mm, $p < 0.0001$) and middle segment (-0.28 HU/10 mm vs. -0.74 HU/10 mm, $p < 0.0001$). Although TAG on S-CTA showed a more rapid reduction pattern than that on C-CTA in the distal segment, TAG values were not significantly different between S-CTA and C-CTA (-1.03 HU/10 mm vs. -0.82 HU/10 mm, $p = 0.002$). The luminal enhancement range and TAG are summarized in Table 4.

연세대학교
YONSEI UNIVERSITY

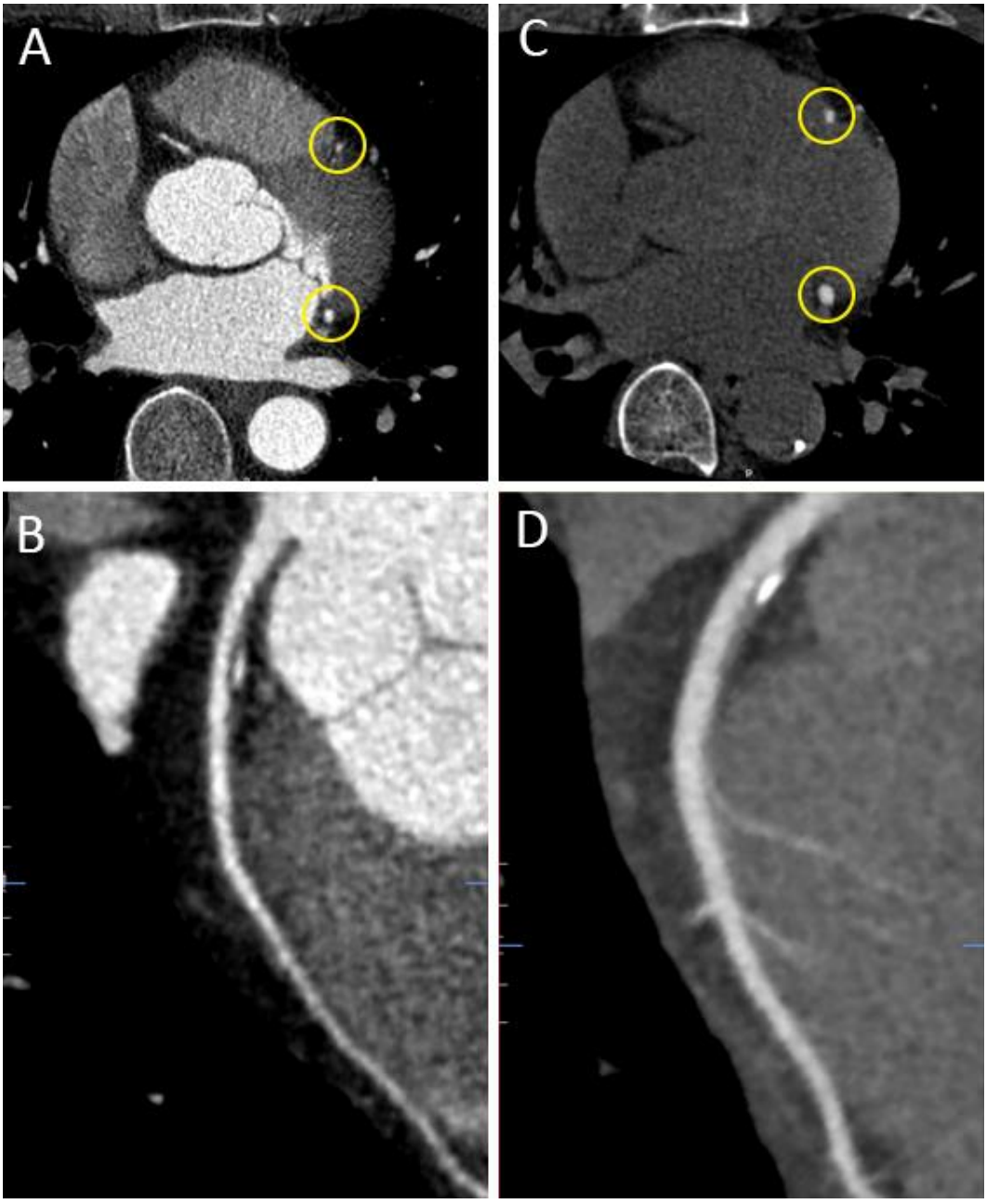

Figure 9 Representative case example of selective computed tomography angiography (S-CTA) and conventional computed tomography angiography (C-CTA) images obtained

연세대학교
YONSEI UNIVERSITY

from the same patient. A: Axial view of C-CTA. B: Axial view of S-CTA. C: Curved multiplanar reconstruction on C-CTA. D: Curved multiplanar reconstruction on S-CTA. Yellow circles indicate contrast-enhanced left anterior descending and left circumflex arteries.

연세대학교
YONSEI UNIVERSITY

C. Image quality analysis.

Image noise was significantly lower on S-CTA than on C-CTA (39.6 ± 10.0 HU vs. 43.9 ± 9.4 HU, $p < 0.0001$). SNR and CNR were significantly higher on S-CTA than on C-CTA (9.3 ± 2.8 HU vs. 8.1 ± 3.0 HU, $p = 0.0040$ for SNR; 9.4 ± 3.2 HU vs. 8.5 ± 2.9 HU, $p = 0.0420$ for CNR).

Table 6 Comparison of quantitative plaque measurements between S-CTA and C-CTA

	PV	%APV
S-CTA	113.2 ± 137.0 mm^3	24.1 ± 13.3%
C-CTA	145.1 ± 135.2 mm^3	26.0 ± 13.8%
Correlation	0.99	0.98
Bland–Altman values (95% confidence intervals)	-5.6, 9.4	-3.2, 19.5

Mean and standard deviation are reported for each measure. PV, plaque volume; %APV, percent aggregate plaque volume; S-CTA, selective computed tomography angiography; C-CTA, conventional computed tomography angiography.

연세대학교
YONSEI UNIVERSITY

D. Plaque volume analysis.

With respect to plaque subtypes, 50% were calcified; 45%, mixed; and 5%, noncalcified. The correlation coefficients and Bland–Altman values with 95% confidence intervals for the comparison of quantitative plaque measurements between S-CTA and C-CTA are shown in Table 6. The p values were significant for PV and %APV, indicating strong correlation and agreement (Table 6).

연세대학교
YONSEI UNIVERSITY

3. Discussion

We evaluated the clinical feasibility of S-CTA as a utilizable CTA modality during coronary catheterization. S-CTA successfully showed luminal enhancement, homogeneous luminal enhancement, and excellent correlation with respect to PV and %APV in the quantitative plaque measurements. In this study, C-CTA was performed with a general dose of iodine (60–90 mL × 370 mg iodine/mL = 22,200–33,300 mg iodine); however, S-CTA was performed with a low dose of iodine (15 mL × 17.19 mg iodine/mL = 258 mg iodine). Although S-CTA was performed with an extremely low dose of iodine, an optimal luminal enhancement of 250–350 HU [25, 26] was achieved. S-CTA showed more homogeneous luminal enhancement than C-CTA in the comparison of TAG. S-CTA was capable of producing a more homogeneous luminal enhancement pattern as the contrast material was directly injected into the intracoronary artery with consistent flow. This homogeneous luminal enhancement led to a significant reduction in image noise and concurrently produced improved SNR and CNR. Furthermore, radiation doses were significantly lower on S-CTA (2.71 ± 1.10 mSv vs. 3.52 ± 2.50 mSv) because S-CTA was performed with relatively small field of view. In the quantitative plaque measurements, PV and %APV on S-CTA showed excellent correlation compared with those on C-CTA despite underestimation of PV and %APV when compared with those on C-CTA. Further studies comparing S-CTA and C-CTA with IVUS are needed to evaluate the clinical feasibility of S-CTA.

연세대학교
YONSEI UNIVERSITY

A. Clinical implications

This combined-modality system enables intraprocedural CTA, which stemmed from the need for neurosurgical field and a new trauma workflow concept with CT scan in the emergency room [41, 42]. The clinical feasibility of intraprocedural CTA during coronary artery intervention was validated in our previous study [43]. In this previous study, S-CTA was performed during intervention for chronic total occlusion (CTO) as an intraprocedural CTA protocol, and we showed that intraprocedural CTA could contribute to successful intervention for CTO. To our knowledge, this study is the first clinical trial on catheter-directed intracoronary contrast-injected imaging protocol during on-site catheterization. Several previous animal studies in which catheters were placed at the superior vena cava and aortic root in a swine model reported the feasibility of catheter-directed contrast-injected CTA. However, a contrast volume reduction of only 50% and 80% was achieved with specialized multi-hole pigtail catheter to spray out the contrast medium. Moreover, clinical validation was not performed in these studies [36, 44]. Conversely, S-CTA showed an iodine dose reduction rate of 99%, and any additional specialized catheter was not necessary as a conventional diagnostic catheter was used in S-CTA. S-CTA might serve as a useful imaging modality for CAD evaluation in patients who present with chronic kidney disease by using a low dose of iodine. In this study, we performed S-CTA in patients with diameter stenosis of 25–99%, and no specific complications occurred after S-CTA. Although S-CTA was performed with an acceptable radiation dose, if S-CTA was applied in multivessel disease, additional radiation exposure would be inevitable. Further optimization of the scan protocol will reduce radiation exposure on S-CTA. Fractional flow reserve (FFR), which represents

연세대학교
YONSEI UNIVERSITY

the pressure differences across a coronary artery stenosis in invasive coronary catheterization, can be calculated from CT scan images by utilizing computational fluid dynamics (CFD) techniques [45, 46]. As S-CTA can produce CTA images that can be utilized for CFD-based FFR calculation, we might obtain information on plaque characteristics and blood pressure through a single S-CTA scan without additional coronary catheterization. Thus, comprehensive evaluation of plaques and lesion-specific ischemia including their characterization might be feasible during on-site coronary catheterization in the near future. However, further investigation is clearly needed to support this contention.

연세대학교
YONSEI UNIVERSITY

B. Study limitations

Our study has some limitations that should be mentioned. First, S-CTA was compared with C-CTA in a relatively small number of plaque lesions. Second, the reference standard for plaque quantification was C-CTA, albeit PV and %APV were only compared between S-CTA and C-CTA. Further study is needed to compare plaque quantification with S-CTA, C-CTA, and IVUS. In conclusion, S-CTA might serve as a useful imaging modality for on-site CAD evaluation and procedure planning for complex lesion, especially when on-site atherosclerotic plaque analysis is required.

연세대학교
YONSEI UNIVERSITY

IV. Deep learning based quantification of stenosis and coronary calcium score from coronary CT Angiography

1. Introduction

Coronary computed tomographic angiography (CTA) has emerged as a reliable noninvasive modality for the diagnosis of coronary artery disease (CAD).[47-50] The improvement of CT image quality over the past decade allows direct evaluation of the entire coronary tree and assessment of both stenosis and coronary plaque.[51-53] Clinical results from CTA currently include only visual stenosis interpretation. Contrast density difference (CDD), a measure of luminal contrast kinetics, has been shown to be related to lesion-specific ischemia by invasive fractional flow reserve.[54] To date, quantitative measurements of stenosis or plaque from CTA are not part of the clinical routine, due to the need for subjective and prohibitively time-consuming manual artery editing.

The time during which CTA matured also coincides with both dramatic increases in computational power and computer graphics capabilities by standard off-the-shelf computer workstations and advances in machine learning, resulting in improved and personalized decision-making in many areas of everyday life. A new class of machine learning algorithms, deep learning, including the well-known convolutional neural networks (CNN), has been shown to be very effective for automated object detection and image classification from a wide range of data.[55-59] Our objective was to evaluate the feasibility of segmentation of coronary lumen and calcified plaque (CP) from CTA using a deep learning or CNN-

연세대학교
YONSEI UNIVERSITY

based segmentation approach, and further, to evaluate quantitative stenosis (and other luminal image biomarkers such as minimum luminal area and CDD) in comparison to expert readers and the Agatston coronary calcium score (CCS) in comparison to non-contrast CT.

연세대학교
YONSEI UNIVERSITY

2. Methods

A. Patients and imaging protocol

In this retrospective study, we included 156 consecutive patients who underwent contrast-enhanced CTA for clinical indications at Cedars-Sinai Medical Center. CTA was performed on a dual-source 64-slice CT scanner (Definition Siemens Medical Solution, Forchheim, Germany) in accordance with societal guidelines. Beta-blockers (orally or intravenously) were administered if necessary to achieve a target patient heart rate of 60- beats/min or less. Prospective and retrospective gating protocols were utilized with a tube voltage of 100 kV in patients with a body mass index (BMI) < 30 kg/m^2 and 120 kV otherwise. Sublingual nitrates were administered just before the scan, and iodinated contrast (65-130 ml) was power injected, followed by a saline flush. Reconstructed data parameters were: 512x512 matrix, 0.5 x 0.5 mm^2 pixel size, 0.6 mm slice thickness, and 0.3 mm slice increment. The study was performed according to the guidelines of Cedars-Sinai Medical Center Institutional Review Board, and all patients provided written informed consent.

연세대학교
YONSEI UNIVERSITY

B. Coronary CTA analysis

The reconstructed CTA were transferred to a central database. Plaque analysis was performed on standard Windows workstations with the semi-automated software tool Autoplaque (version 2.0, Cedars-Sinai Medical Center, Los Angele, CA, USA)[52] by expert readers with level III or higher certification in cardiac CT. For each scan, the reader first placed a circular region-of-interest in the aortic root and scan-specific plaque thresholds were computed by the software as described previously.[60, 61] Quantitative measurements were made in each coronary segment using a standard 17-segment model[62] (SCCT guidelines) up to a luminal diameter limit ≥ 1.5 mm. Plaque quantification was performed with adaptive algorithms that are scan-specific, as previously described.[60, 61] Minimal lumen area (MLA) CP volume of the lesion were measured.[60, 61] Quantitative percent diameter stenosis (DS) was calculated by dividing the narrowest lumen diameter by the average of two normal non-diseased reference cross-sections. CDD was defined as the maximum percent difference in contrast densities (luminal contrast density or attenuation per unit area), with respect to the proximal reference cross-section (with no disease). If the manual adjustments were needed, edits were made using the standardized correction options in the software, which allows for editing of vessel wall, lumen, calcified plaque and adjustment of plaque thresholds. Interobserver variability was evaluated in a subset of 20 patients by two independent readers. CCS is measured from non-contrast CT.[63] From CTA, Agatston score from CP volume was calculated using a regression relation, similar to our previous study.[64] For calculating CCS from CTA, 3.0326 Agatston units/mm^3 was used as a conversion factor and systematically compared to Agatston calcium scores measured from non-contrast CT.

연세대학교
YONSEI UNIVERSITY

C. Data preparation for convolutional neural networks

The lesion segments were reconstructed to straightened views by using the extracted centerlines. The input of the convolutional networks was the extracted from 2-D cross-sectional image, while the expert annotations were defined as the target references of the convolutional networks. We evaluated 2 sets of plaque thresholds for the input: the scan-specific thresholds used in the software and a general threshold evaluated from a separate training cohort of 50 patients acquired at the same site with the same acquisition parameters (-10 to 200 HU for NCP, lumen 201 HU to 499 HU, CP ≥500 HU). In this study, the expert annotations had three labels as follows: background, contrast-enhanced lumen, and CP. We divided the target annotation into two types: 1) background and foreground (lumen + CP annotations); and 2) background and foreground (CP annotation only). Therefore, we prepared 2 sets of 4 channels input (CTA cross-sections preprocessed with the 4 HU threshold ranges), and 2 classes target (background and foreground). Two datasets were trained separately, one for each target.

연세대학교
YONSEI UNIVERSITY

D. Deep Learning architecture

A convolutional network architecture inspired by M-Net[65] was designed. M-Net is an end-to-end CNN architecture for segmenting brain structures from Magnetic Resonance (MR) Images, and it was inspired by U-Net.[55, 56] M-Net was proposed to overcome the drawbacks of U-Net. U-Net was performed on 256 × 256 × 256 MR volume images, and it consisted of continuative 2D convolutional layers.[55] Therefore, it has the disadvantage of being unable to use 3-D information. A 3-D U-Net consisting of serial 3-D convolutional layers was proposed to utilize 3-D information. However, this architecture requires a large memory to train this volume of images, even when using down-sampled resolution images as inputs.[56] M-Net has a 3D-to-2D convolutional layer in front of the U-Net architecture to utilize 3D information memory efficiently. Another advantage of M-Net is the leg-like layers on the front and back of U-Net, and its two side paths provide functional deep-supervision. However, 3-dimensional input was reconstructed with a stack of 2D images, and the number of slice images that must be accumulated to produce a 3-dimensional input was empirically determined. In this study, we used a straightened curved planar reformation image, which was reconstructed with the center line of the coronary artery, thus creating inconsistencies in the length of the lesion. Therefore, 2D U-Net is more suitable for this study. We included two side pathways to take advantage of the M-Net. Our architecture is a 2D CNN without a 3D-to-2D converter. Our convolutional architecture is the combination of the encoding and decoding steps. The encoding step has 5 sets of compression layers. A compression layer set has 2 convolutional layers of size 3 × 3 and a max-pooling layer of size 2 × 2. These compression layers produce half the size of the input dimension using contextual

연세대학교
YONSEI UNIVERSITY

information. The number or convolutional filters was gradually increased to avoid information loss as information was reduced by max-pooling. Decompression is symmetric to the compression step by replacing max-pooling with up-sampling to recover dimension. The feature maps from each convolution layer is concatenated to the corresponding next convolution layer to enable precise feature localization. Skip connection was introduced to create two side pathways. These side pathways help the model to be trained with sufficient information. Figure 10 shows the proposed CNN architecture. All convolution layers are activated with the parametric rectified linear unit to ensure fast convergence of the convolutional network.[66] Batch normalization was applied to accelerate the training of the convolutional networks.[67] Dropout probability was set to p = 0.5 to prevent overfitting.[68] The final layer is processed by a 1 × 1 convolution layer with 2 channels (foreground, background) and pixel-wise SoftMax, which allows the probability of 2 classes. The final segmentation labels were assigned to the classes with maximum probability for every pixel. We combined binary cross-entropy (Eq. 1) and Jaccard index (Eq. 2), also known as intersection over the union, to compare the similarities and diversities of the sample sets.

$$H = -\frac{1}{n}\sum_{i=1}^{n}[y\log(\widehat{y}) + (1-y)\log(1-\widehat{y})] \tag{1}$$

$$J_m(y,\widehat{y}) = \frac{1}{n}\sum_{i=1}^{n}\frac{y_i \cdot \widehat{y_i}}{y_i + \widehat{y_i} - y_i \cdot \widehat{y_i}} \tag{2}$$

Thus, the joint loss function is defined as follows:

연세대학교
YONSEI UNIVERSITY

$$L = H - \log J_m \tag{3}$$

We used an Adam optimizer to optimize the loss function, and the convolutional architecture was trained for 70 epochs.

연세대학교
YONSEI UNIVERSITY

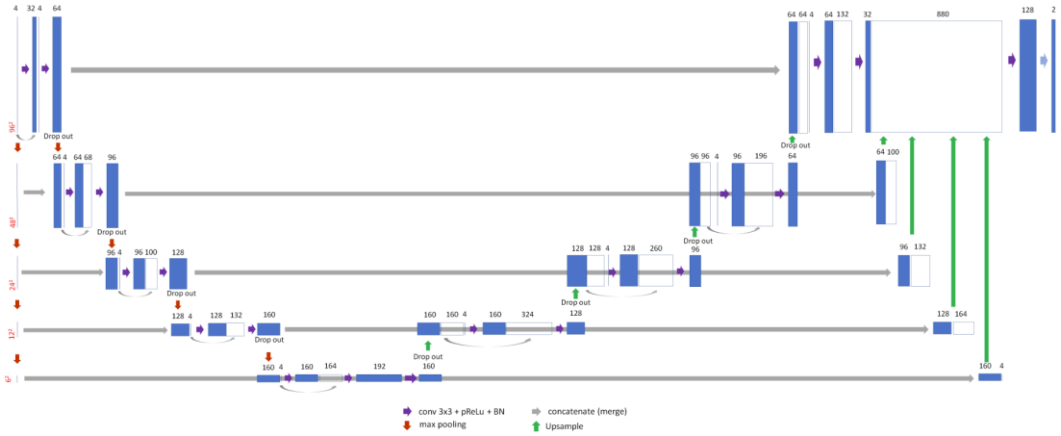

Figure 10 Proposed convolutional neural networks architecture.

연세대학교
YONSEI UNIVERSITY

E. Cross-validation

The entire experiments were performed using 10-fold cross-validation, for robust non-biased evaluation. During validation, all the lesion cases were randomly shuffled and split into 1/10 of the aggregate data. The model trained with 9/10 of the data (642 lesions) and then tested against the remaining subset (remaining 72 lesions). The validation was repeated 10 times and results concatenated until the entire dataset was segmented. MLA, DS, CDD, and CP volumes were computed from both expert and deep learning for each lesion and exported to Excel.

연세대학교
YONSEI UNIVERSITY

F. Validation for plaque quantification

To validate plaque quantification performance of our deep learning model, we compared CP volume from CTA and IVUS. We utilized 10 lesion segments that were performed CTA, S-CTA, and IVUS for the validation. CP volume from IVUS was manually measured by expert IUVS reader in a blind manner, and CP volume from CTA and S-CTA was measured with proposed deep learning model at the matched location.

연세대학교
YONSEI UNIVERSITY

G. Deep learning on Selective CTA

To validate the feasibility of the S-CTA as an adjunctive imaging modality for CAD evaluation, the proposed deep learning model was utilized with S-CTA to measure CP volume. The model was trained with 716 lesion segments, and these segments were not related with S-CTA or C-CTA. The trained deep learning model was applied on 10 S-CTA/C-CTA/IUVS paired volume datasets, and the CP volume was measured. The measured CP volume was compared with the CP volume from IVUS.

연세대학교
YONSEI UNIVERSITY

H. Statistical analysis

The primary end-point of this study was the performance of the deep learning compared to the evaluation by the expert reader. Statistical analysis was performed using Excel add-in Analyse-it software (Analyse-it, Leeds, UK). Continuous variables were expressed as mean ± standard deviation or median and interquartile range (IQR). Deep learning and expert quantifications were systematically compared, using the Spearman correlation coefficient and Bland-Altman plots and paired Wilcoxon rank-sum test. Deep learning performance was also evaluated with dice similarity coefficient (DSC), as a measure of overlap between expert and deep learning. This is computed by:

$$DSC = 2TP/(2TP+FP+FN),$$

Where TP (true positive) is the number of correctly positively annotated voxels, FP (false positive) is the number of incorrectly positively annotated, and FN (false negative) is the number of incorrectly negatively annotated voxels. A p-value of < 0.05 was considered statistically significant.

연세대학교
YONSEI UNIVERSITY

3. Results

A. Patient characteristics

The patient characteristics are presented in Table 7. The study cohort included 113 males (73%), and the mean age was 66 ± 10 years. Body mass index, risk factors, and history of coronary artery disease at the time of CTA examination are listed in Table 7.

연세대학교
YONSEI UNIVERSITY

Table 7 Patient characteristics

Number of patients	156
Age, years (mean ± SD)	66 ± 10
Male, n (%)	113 (73)
Body mass index, kg/m^2	27 ± 5
Risk factors and history of coronary artery disease	
Diabetes, n (%)	27 (17)
Hypertension, n (%)	81 (52)
Hyperlipidemia, n (%)	110 (71)
Current smoker, n (%)	11 (7)
Previous myocardial infarction, n (%)	2 (1)
Symptoms	
Typical angina, n (%)	8 (5)
Atypical angina, n (%)	12 (8)
Nonanginal chest pain, n (%)	45 (29)
Shortness of breath, n (%)	72 (46)
Asymptomatic, n (%)	55 (35)

연세대학교
YONSEI UNIVERSITY

B. Experiments

The proposed model was trained for 70 epochs; we chose the best performance model during the training. We tested its performance according to the general threshold model and the scan-specific threshold model separately. In the training process, we measured training loss, training accuracy, validation loss, and validation accuracy. We also measured dice coefficient on the test dataset. Tables 8–11 show the training results according to the general threshold model and the scan-specific threshold model. Figure 11 shows a representative example for the training procedure.

연세대학교
YONSEI UNIVERSITY

Table 8 Training results on lumen model with general threshold dataset.

	Lumen model				
	Best Epoch	Training Loss	Training Acc	Validation loss	Validation Acc
0_fold	60	0.0226	0.9954	0.0242	0.9959
1_fold	61	0.0236	0.9958	0.0237	0.9959
2_fold	62	0.0222	0.9961	0.0237	0.9959
3_fold	61	0.0237	0.9957	0.0250	0.9958
4_fold	65	0.0262	0.9960	0.0241	0.9958
5_fold	68	0.0245	0.9955	0.0242	0.9959
6_fold	50	0.0260	0.9954	0.0252	0.9957
7_fold	70	0.0245	0.9955	0.0242	0.9959
8_fold	48	0.0255	0.9955	0.0253	0.9956
9_fold	70	0.0249	0.9956	0.0231	0.9960
Aver-age		0.0244	0.9957	0.0243	0.9958

Acc = Accuracy

연세대학교
YONSEI UNIVERSITY

Table 9 Training results on calcified plaque model with general threshold dataset.

	Calcified plaque model				
	Best Epoch	Training Loss	Training Acc	Validation loss	Validation Acc
0_fold	29	0.0223	0.9982	0.0077	0.9986
1_fold	30	0.0115	0.9983	0.0069	0.9988
2_fold	30	0.0196	0.9981	0.0085	0.9985
3_fold	29	0.0114	0.9986	0.0071	0.9987
4_fold	59	0.0055	0.9990	0.0063	0.9989
5_fold	59	0.0047	0.9992	0.0060	0.9989
6_fold	40	0.0231	0.9983	0.0068	0.9987
7_fold	29	0.0234	0.9983	0.0068	0.9988
8_fold	50	0.0100	0.9995	0.9984	0.9988
9_fold	50	0.0110	0.9986	0.0073	0.9987
Aver-age		0.0142	0.9986	0.1062	0.9987

Acc = Accuracy

연세대학교
YONSEI UNIVERSITY

Table 10 Training results on lumen model with scan-specific threshold dataset.

	Lumen model				
	Best Epoch	Training loss	Training Acc	Validation loss	Validation Acc
0_fold	36	0.0239	0.9958	0.0238	0.9959
1_fold	37	0.0229	0.9959	0.0233	0.9960
2_fold	38	0.0218	0.9961	0.0237	0.9960
3_fold	36	0.0252	0.9955	0.0236	0.9958
4_fold	39	0.0235	0.9958	0.0231	0.9960
5_fold	34	0.0245	0.9956	0.0242	0.9959
6_fold	37	0.0229	0.9958	0.0230	0.9960
7_fold	33	0.0252	0.9952	0.0244	0.9959
8_fold	27	0.0457	0.9948	0.0273	0.9954
9_fold	40	0.0219	0.9961	0.0235	0.9960
Average		0.0257	0.9957	0.0240	0.9959

Acc = Accuracy

연세대학교
YONSEI UNIVERSITY

Table 11 Training results on calcified plaque model with scan-specific threshold dataset.

	Calcified plaque model				
	Best Epoch	Training Loss	Training Acc	Validation loss	Validation Acc
0_fold	40	0.0059	0.9990	0.0060	0.9989
1_fold	40	0.0052	0.9990	0.0054	0.9990
2_fold	40	0.0052	0.9990	0.0054	0.9990
3_fold	39	0.0045	0.9992	0.0068	0.9989
4_fold	36	0.0047	0.9992	0.0055	0.9990
5_fold	43	0.0053	0.9990	0.0055	0.9990
6_fold	39	0.0056	0.9990	0.0057	0.9990
7_fold	38	0.0053	0.9990	0.0057	0.9990
8_fold	37	0.0064	0.9991	0.0058	0.9990
9_fold	38	0.0508	0.9991	0.0569	0.9990
Aver-age		0.0099	0.9991	0.0109	0.9990

Acc = Accuracy

연세대학교
YONSEI UNIVERSITY

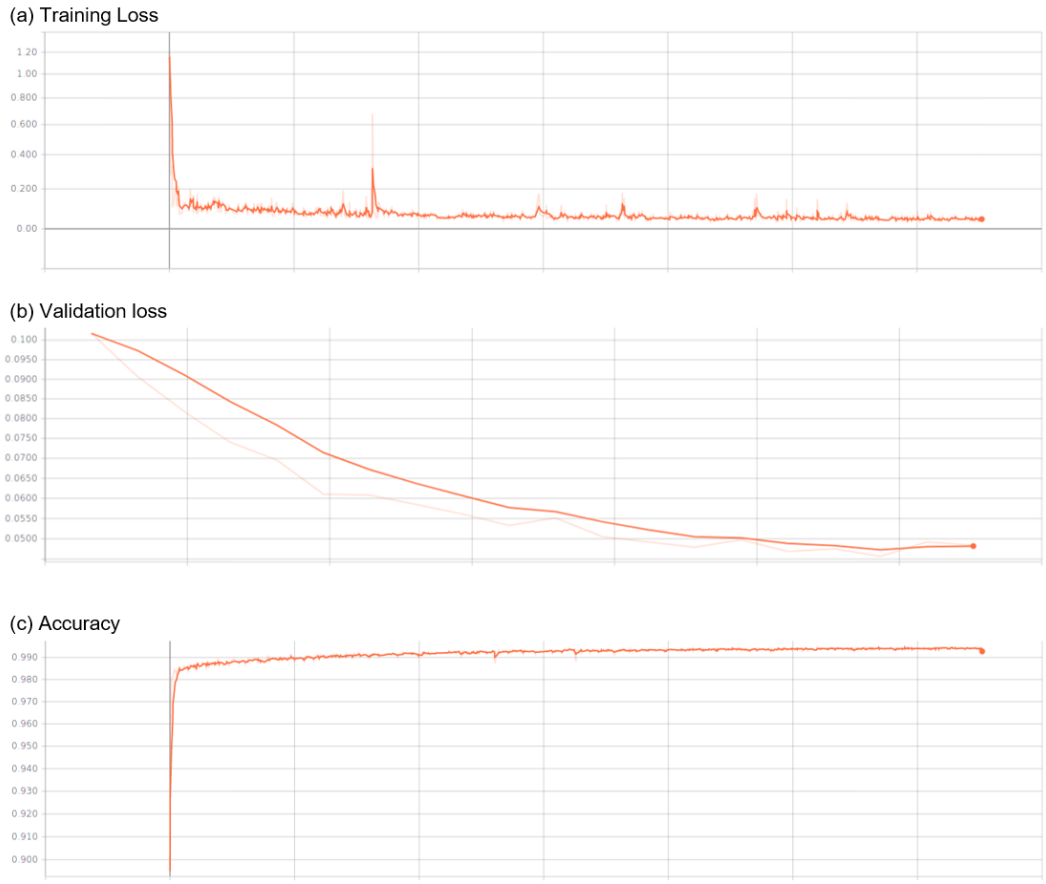

Figure 11 A representative example of training procedure. This image was captured on Tensor board.

연세대학교
YONSEI UNIVERSITY

B. Quantitative CTA measures

Out of 716 lesion segments, MLA, DS, CDD, and CP volume were measured. The typical time for computation was <32 seconds on a standard Windows workstation (mean 31.1 ± 21.0 seconds). Figure 12 shows a representative case example of quantitative plaque analysis from our study. Figures 13-16 show the correlations and Bland-Altman plots for the quantitative measures MLA, DS, CDD, CP volume. Overall, both general threshold and scan-specific threshold quantifications showed excellent correlation and agreement for MLA, DS, CDD, and CP volume with expert quantification. The scan-specific threshold quantification demonstrated Spearman rank coefficients from 0.96 to 0.99, and the general threshold quantification showed rank coefficients from 0.86 to 0.91.

연세대학교
YONSEI UNIVERSITY

C. Plaque quantification validation

We compared the CP volumes from CTA with the reference volumes from IVUS. Table 12 shows the measured plaque volumes. Our deep learning model measured CP volumes that were close to the reference CP volumes (mean 144 mm^3 vs. 151 mm^3, CTA, IVUS, respectively).

Table 12 Calcified plaque volume from C-CTA and IVUS

Case #	Calcified plaque volume (mm^3)	
	CTA	IVUS
00	288	313
01	60	81
02	256	234
03	135	119
04	82	88
05	94	171
06	99	103
07	179	184
08	102	58
09	145	161
average	144	151

연세대학교
YONSEI UNIVERSITY

D. Plaque quantification validation for selective CTA

We compared the CP volumes from S-CTA, C-CTA, and IVUS and calculated the difference between the CP volumes. The proposed deep learning model measured CP volumes that were close to the reference CP volumes (mean 142 mm^3 vs. 151 mm^3, CTA, IVUS, respectively). Volume differences of S-CTA − IUVS and C-CTA − IUVS were calculated. The mean difference from S-CTA − IVUS showed less difference than C-CTA − IVUS. The maximum volume difference between S-CTA and IUVS was 26 mm^3, but the maximum difference between C-CTA and IVUS was 77 mm^3 (case number 05). Table 13 shows the CP volume measurement results.

연세대학교
YONSEI UNIVERSITY

Table 13 Calcified plaque comparison between S-CTA/C-CTA and IUVS

Case #	Calcified plaque volume (mm^3)			Volume difference (mm^3)	
	S-CTA	C-CTA	IVUS	S-CTA - IVUS	C-CTA - IVUS
00	302	288	313	11	25
01	68	60	81	13	21
02	218	256	234	16	22
03	113	135	119	6	16
04	79	82	88	9	6
05	145	94	171	26	77
06	94	99	103	9	4
07	176	179	184	8	5
08	64	102	58	6	44
09	167	145	161	6	16
aver-age	142	144	151	11	24

연세대학교
YONSEI UNIVERSITY

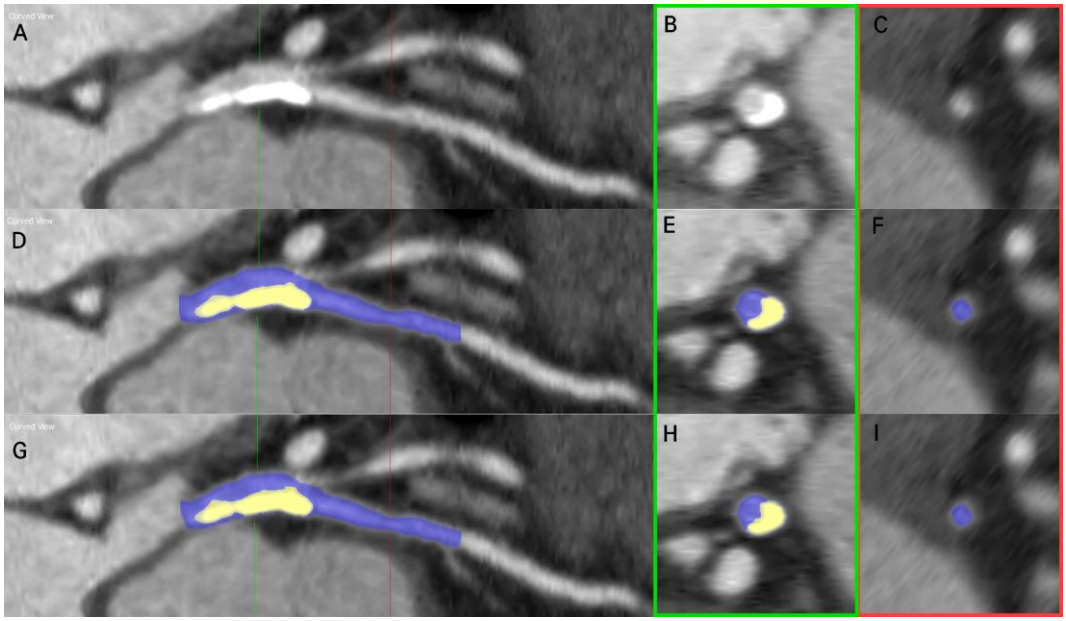

Figure 72 Representative case example of lumen and calcified plaque quantification in the proximal to mid left anterior descending artery (LAD). (A) Curved planar reformation view on the lesion. (B) The cross-sectional image at the level of obstructive lesion (indicated in green). (C) The cross-sectional image at the level of minimal lumen area (indicated in red). (D) and (E), and (F) are expert quantification of the lesion. (G) and (H), and (I) are deep learning quantification of the lesion. Blue indicates contrast-enhanced lumen and yellow indicates calcified plaque. In expert quantification, MLA: 2.9 mm^2, DS: 43.7%, CDD: 8.1%, and CP volume 71.6 mm^3. Compared to deep learning quantification, MLA: 2.9 mm^2, DS: 43.1%, CDD: 7.6%, and CP volume 86.5 mm^3.

연세대학교
YONSEI UNIVERSITY

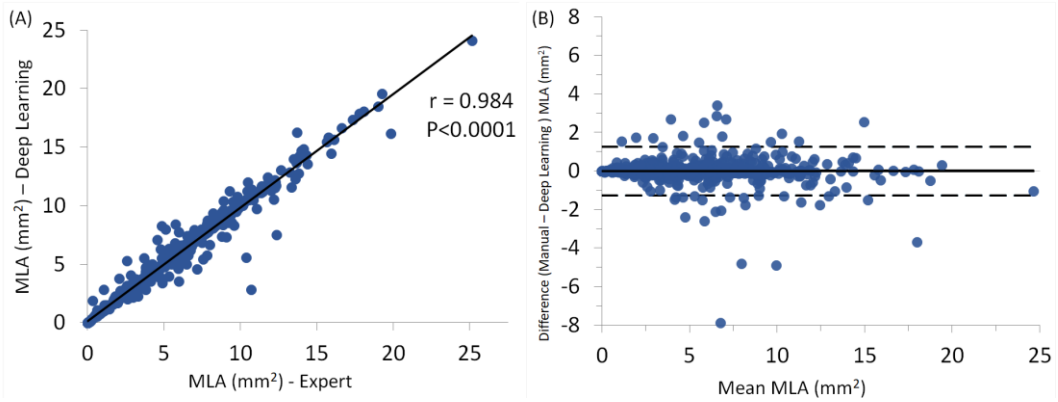

Figure 83 (A) Spearman correlation and (B) Bland-Altman plots on minimal lumen area evaluation between deep learning and expert quantification. A strong Spearman correlation was observed r = 0.984, and 95% of limits agreements were -1.2 to 1.2 mm^2.

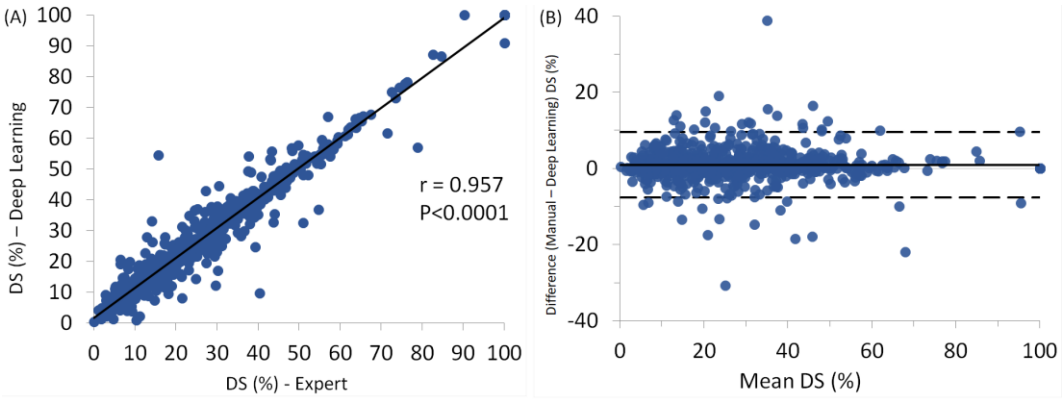

Figure 94 (A) Spearman correlation and (B) Bland-Altman plots on percent diameter stenosis evaluation between deep learning and expert quantification. A strong Spearman correlation was observed r = 0.957. The 95% of limits agreements were -7.7 to 9.5 %.

연세대학교
YONSEI UNIVERSITY

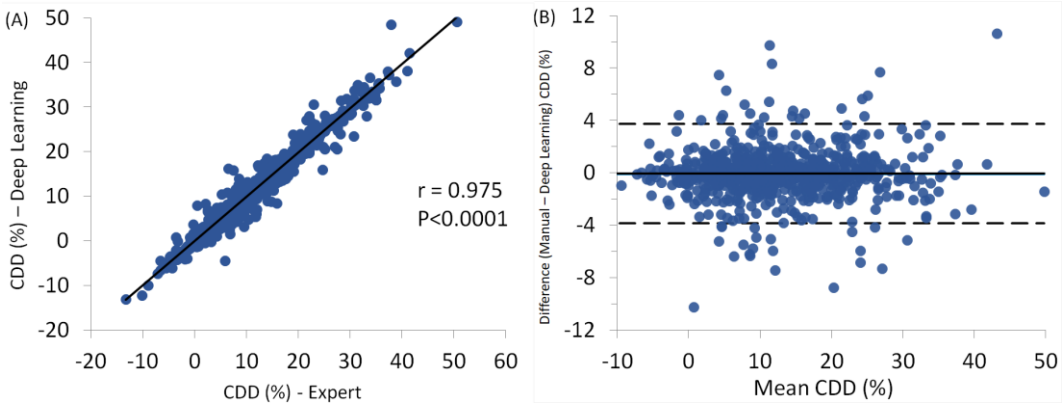

Figure 105 (A) Spearman correlation and (B) Bland-Altman plots on percent contrast density difference evaluation between deep learning and expert quantification. A strong Spearman correlation was observed r = 0.975, and 95% of limits agreements were -3.9 to 3.8 %.

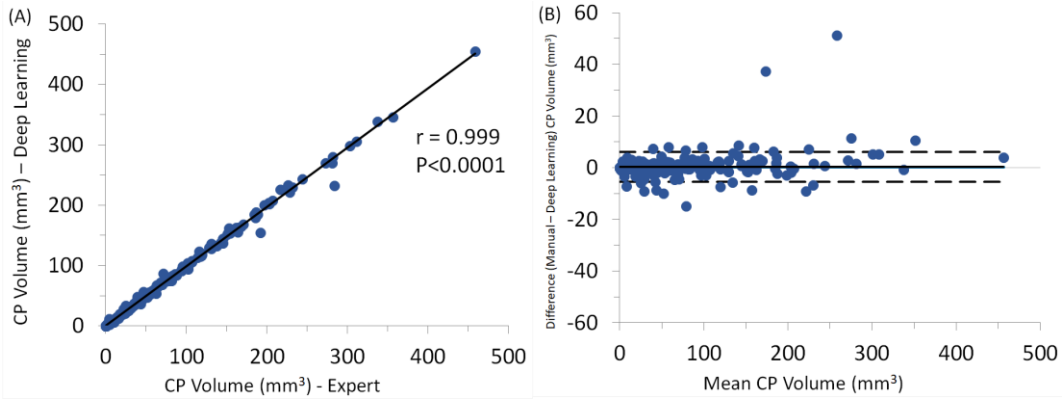

Figure 116 (A) Spearman correlation and (B) Bland-Altman plots on calcified plaque volume evaluation between deep learning and expert quantification. A strong Spearman correlation was observed r = 0.999, and 95% of limits agreements were -5.5 to 6.1 mm^3.

Table 14 shows the DSC results for lumen and CP annotations (scan-specific threshold)

연세대학교
YONSEI UNIVERSITY

during the 10-fold cross-validation. Table 15 shows the median and IQR of the imaging biomarkers with the p-values for pairwise comparison between deep learning and expert quantification. The correlation coefficients and Bland-Altman 95% confidence intervals for the comparison of quantitative plaque measures using general or scan-specific threshold are shown in Table 15.

연세대학교
YONSEI UNIVERSITY

Table 14 Dice similarity coefficient between expert and deep learning annotations for 10-fold cross-validation

No. of fold	DSC for Lumen	DSC for CP
0_fold	0.96	0.91
1_fold	0.96	0.91
2_fold	0.96	0.90
3_fold	0.95	0.91
4_fold	0.96	0.90
5_fold	0.95	0.88
6_fold	0.96	0.92
7_fold	0.95	0.89
8_fold	0.95	0.90
9_fold	0.95	0.91
Mean DSC	0.95	0.90

Dice similarity coefficient (DSC) evaluates the segmentation performance. The value of the DSC ranges from 0 to 1, where 0 means that there is no similarity and 1 means that there is complete similarity.

연세대학교
YONSEI UNIVERSITY

While the p-values were significant for all the biomarkers for the general thresholds, MLA and CDD were not significantly different from expert quantification for scan-specific threshold only (P=0.6786 and P=0.2996, respectively). From the Bland-Altman plots in Figures 13-16, for all the quantitative measures, the 95% limits of agreement for the general thresholds were wider by 200-300%, indicating worse agreement with the expert reader (Table 15). Even for scan-specific thresholds, however, there were few outliers, and these could be attributed to ostial lesions particularly at the ostium of the Left Main artery, performance of deep learning was lower/less accurate in these lesions. Table 16 shows the absolute difference between 2 expert readers for the quantitative parameters. For all the quantitative parameters, 95% limits of agreement for the deep learning method were within range of the differences between 2 expert readers.

연세대학교
YONSEI UNIVERSITY

Table 15 Comparison of deep learning vs expert evaluation for measured parameters (median and interquartile ranges are reported for each measure)

	Plaque thresholds utilized	
Quantitative parameter	*General*	Scan-specific
Minimal Lumen Area (mm2)		
Deep Learning Evaluation	*4.2 (2.5 - 6.4)*	4.4 (2.6 - 6.6)
Expert (manual) Evaluation	*4.4 (2.6 - 6.6)*	4.4 (2.6 - 6.6)
P – value	*0.0043*	0.6786[+]
Correlation	*0.915*	0.984
Bland Altman (95% limits)	*-2.7, 2.3*	-1.3, 1.3
CP volume (mm^3)		
Deep Learning Evaluation	*10.1 (1.4 - 32.0)*	10.2 (1.7 - 33.9)
Expert (manual) Evaluation	*10.3 (1.7 - 33.9)*	10.3 (1.7 - 33.9)
P – value	*<0.0001*	<0.0001
Correlation	*r = 0.859*	r = 0.999
Bland Altman (95% limits)	*-33.4, 31.6*	-5.5, 6.1
Diameter Stenosis (%)		
Deep Learning Evaluation	*28.2 (17.3 - 39.6)*	26.6 (16.3 - 38.5)
Expert (manual) Evaluation	*26.0 (15.1 - 37.9)*	26.0 (15.1 - 37.9)
P – value	*<0.0001*	<0.0001
Correlation	*r = 0.873*	r = 0.957
Bland Altman (95% limits)	*-18.3, 23.0*	-7.7, 9.5
Contrast density difference (%)		
Deep Learning Evaluation	*13.2 (7.6 - 21.4)*	11.2 (5.6 - 18.4)
Expert (manual) Evaluation	*11.6 (6.0 - 18.3)*	11.6 (6.0 - 18.3)
P – value	*<0.0001*	0.2996[+]

연세대학교
YONSEI UNIVERSITY

Correlation	*r = 0.873*	r = 0.975
Bland Altman (95% limits)	*-8.0, 12.0*	-3.9, 3.8

Generic indicates that general threshold applied CNN model, Scan-specific indicates that scan-specific threshold applied CNN model. Median (1^{st} quartile – 3^{rd} quartile), P-value is Wilcoxon rank sum test and $p < 0.05$ is considered as significant. $^{+}$**For MLA and CDD, pairwise differences were significantly not different for the scan-specific method, indicating equivalence.**

연세대학교
YONSEI UNIVERSITY

Table 16 Inter-observer variability (absolute difference) in quantitative measures

Quantitative parameters	
Minimal Lumen Area (mm2)	
Mean	1.5 ± 2.2
95% CI	0 - 6.3
CP volume (mm^3)	
Mean	5.6 ± 19.9
95% CI	0 - 51.1
Diameter Stenosis (%)	
Mean	11.6 ± 11.8
95% CI	1.0 - 36.0
Contrast density difference (%)	
Mean	2.6 ± 2.6
95% CI	0 – 7.9

For all quantitative parameters, 95% limits of agreement for the deep learning method were within range of the differences between 2 expert readers.

연세대학교
YONSEI UNIVERSITY

E. Coronary calcium score from quantitative CTA

CCS was calculated from CTA from CP volume. In 47 patients where non-contrast CT data was available, CCS derived from CP volume showed strong correlation with CCS from non-contrast CT (Spearman rank correlation=0.8784, $p<0.0001$) and did not differ significantly [484.3 ± 633.5 vs. 514.2 ± 689.4, $p=0.11$].

연세대학교
YONSEI UNIVERSITY

4. Discussion

In this study, we evaluated the feasibility of deep learning for quantitative coronary artery analysis and showed that clinically relevant parameters such as MLA, DS, CDD, and CP volume could be accurately measured from CTA. We further showed that the coronary calcium score could be measured from contrast-enhanced CTA following such measurement. Our deep learning model successfully captured intrinsic features of contrast-enhanced lumen and CP from CTA. To the best of our knowledge, this has not been demonstrated before. We also evaluated two sets of plaque thresholds for measurement of MLA, DS, CDD, and CP volume. These two methods showed a strong correlation with expert quantification, with scan-specific thresholds yielding more accurate results. While this requires minor manual interactions (the placing of a standard region-of-interest at the aortic root), these are not time-consuming tasks and with further development of this new approach, could potentially become fully automated.

Deep learning, a particular form of machine learning, has been recently applied to other noninvasive imaging, both by our group and others; our study is in line with and extends these studies. Myocardial perfusion imaging with Single Photon Emission Computed Tomography can be automatically interpreted by deep learning.[59] We have shown that epicardial adipose tissue, a metabolically active fat depot directly surrounding the coronary arteries, can be quantified automatically using deep learning from non-contrast CT.[57] Deep learning can potentially identify hemodynamically significant coronary stenosis by analyzing the left ventricle from CTA.[58] Our deep learning method allows rapid measurement (1.7

연세대학교
YONSEI UNIVERSITY

± 1.1 seconds per lesion) of quantitative stenosis parameters such as MLA, DS, and CDD, as well as plaque features such as CP volume and coronary calcium score derived from CTA. While currently these parameters are not included in standard clinical reporting, by utilizing our novel approach such quantitative data could become routinely available. CDD is a quantitative measure of luminal contrast kinetics, and our recent work has shown that this parameter is related to both lesion-specific ischemia[54, 69] and cardiac death.[70] Our study showed that there is no difference between manual evaluation and deep learning evaluation of CDD. The coronary calcium score is a strong predictor of major adverse cardiovascular events; however, it is typically not quantified from contrast-enhanced CTA.

In the validation, we compared CP volumes from S-CTA and C-CTA with IVUS. We used only 10 test volumes paired with C-CTA, S-CTA, and IVUS. It was not enough to calculate statistical significance but we found that CP volume from S-CTA was closer to the reference volumes. S-CTA produced hologenetic luminal enhancement, and it caused better quantification performance even though we applied same CNN architecture and same parameters. On-site evaluation of S-CTA is possible with the proposed CNN model.

We can obtain the calcium score without additional non-contrast CT scan. Once incorporated into the software, such deep learning models can enhance CTA clinical report by reporting stenosis grades, and the presence of obstructive stenosis, as well as the coronary calcium score. Further, change in quantitative stenosis could provide a simple measure of total plaque progression in serial studies[71] and allow clinicians to monitor progression or regression of a disease.

연세대학교
YONSEI UNIVERSITY

This study has some limitations. Our deep learning quantification was still semi-automatic, with minor manual operations required from the observer. Since the model was performed on a designated lesion segment, the observer set the proximal and distal limits of the lesion. While scan-specific plaque thresholds, as applied in this study, showed more accurate agreement with expert readers, it can be considered as a bias. In this feasibility study, we did not include non-calcified plaque measurement; for this task, a more complex deep-learning architecture, with shape regularization of the vessel wall,[57] similar to the expert reader annotations, may be necessary.

5. Conclusions

Our deep learning-based method enables quantitative measurement of coronary artery disease and coronary calcium score accurately and may enhance clinical reporting.

연세대학교
YONSEI UNIVERSITY

REFERENCES

1. Ryan TJ. The coronary angiogram and its seminal contributions to cardiovascular medicine over five decades. Circulation. 2002;106(6):752-6.
2. Levin DC. Invasive evaluation (coronary arteriography) of the coronary artery disease patient: clinical, economic and social issues. Circulation. 1982;66(5 Pt 2):III71-9.
3. Nissen SE, Gurley JC, Grines CL, Booth DC, McClure R, Berk M, et al. Intravascular ultrasound assessment of lumen size and wall morphology in normal subjects and patients with coronary artery disease. Circulation. 1991;84(3):1087-99.
4. Bezerra HG, Costa MA, Guagliumi G, Rollins AM, Simon DI. Intracoronary optical coherence tomography: a comprehensive review clinical and research applications. JACC Cardiovasc Interv. 2009;2(11):1035-46.
5. Hur SH, Kang SJ, Kim YH, Ahn JM, Park DW, Lee SW, et al. Impact of intravascular ultrasound-guided percutaneous coronary intervention on long-term clinical outcomes in a real world population. Catheter Cardiovasc Interv. 2013;81(3):407-16.
6. Alfonso F, Flores A, Escaned J, Sanmartin M, Hernandez R, Fernandez-Ortiz A, et al. Pressure wire kinking, entanglement, and entrapment during intravascular ultrasound studies: a potentially dangerous complication. Catheter Cardiovasc Interv. 2000;50(2):221-5.

연세대학교
YONSEI UNIVERSITY

7. Vanhoenacker PK, Heijenbrok-Kal MH, Van Heste R, Decramer I, Van Hoe LR, Wijns W, et al. Diagnostic performance of multidetector CT angiography for assessment of coronary artery disease: meta-analysis. Radiology. 2007;244(2):419-28.

8. Hamon M, Biondi-Zoccai GG, Malagutti P, Agostoni P, Morello R, Valgimigli M, et al. Diagnostic performance of multislice spiral computed tomography of coronary arteries as compared with conventional invasive coronary angiography: a meta-analysis. J Am Coll Cardiol. 2006;48(9):1896-910.

9. Schroeder S, Kuettner A, Leitritz M, Janzen J, Kopp AF, Herdeg C, et al. Reliability of differentiating human coronary plaque morphology using contrast-enhanced multislice spiral computed tomography: a comparison with histology. J Comput Assist Tomogr. 2004;28(4):449-54.

10. Motoyama S, Sarai M, Narula J, Ozaki Y. Coronary CT angiography and high-risk plaque morphology. Cardiovasc Interv Ther. 2013;28(1):1-8.

11. Schwarz F, Hinkel R, Baloch E, Marcus RP, Hildebrandt K, Sandner TA, et al. Myocardial CT perfusion imaging in a large animal model: comparison of dynamic versus single-phase acquisitions. JACC Cardiovasc Imaging. 2013;6(12):1229-38.

12. Stahli BE, Bonassin F, Goetti R, Kuest SM, Frank M, Altwegg LA, et al. Coronary computed tomography angiography indicates complexity of percutaneous coronary interventions. J Invasive Cardiol. 2012;24(5):196-201.

13. Kubo T, Maehara A, Mintz GS, Doi H, Tsujita K, Choi SY, et al. The dynamic nature of coronary artery lesion morphology assessed by serial virtual histology

연세대학교
YONSEI UNIVERSITY

intravascular ultrasound tissue characterization. J Am Coll Cardiol. 2010;55(15):1590-7.

14. Stone GW, Maehara A, Lansky AJ, de Bruyne B, Cristea E, Mintz GS, et al. A prospective natural-history study of coronary atherosclerosis. N Engl J Med. 2011;364(3):226-35.

15. Boogers MJ, Broersen A, van Velzen JE, de Graaf FR, El-Naggar HM, Kitslaar PH, et al. Automated quantification of coronary plaque with computed tomography: comparison with intravascular ultrasound using a dedicated registration algorithm for fusion-based quantification. Eur Heart J. 2012;33(8):1007-16.

16. Heo R, Park H-B, Lee BK, Shin S, Arsanjani R, Min JK, et al. Optimal boundary detection method and window settings for coronary atherosclerotic plaque volume analysis in coronary computed tomography angiography: comparison with intravascular ultrasound. European radiology. 2015:1-9.

17. Sun J, Hu J, Luo D, Markatou M, Wang F, Edabollahi S, et al. Combining knowledge and data driven insights for identifying risk factors using electronic health records. AMIA Annu Symp Proc. 2012;2012:901-10.

18. Escudero J, Ifeachor E, Zajicek JP, Green C, Shearer J, Pearson S, et al. Machine learning-based method for personalized and cost-effective detection of Alzheimer's disease. IEEE Trans Biomed Eng. 2013;60(1):164-8.

19. Wu J, Roy J, Stewart WF. Prediction modeling using EHR data: challenges, strategies, and a comparison of machine learning approaches. Med Care. 2010;48(6 Suppl):S106-13.

연세대학교
YONSEI UNIVERSITY

20. Gidaris S, Komodakis N. Object detection via a multi-region and semantic segmentation-aware cnn model. Proceedings of the IEEE International Conference on Computer Vision, 2015. 1134-42.

21. Krizhevsky A, Sutskever I, Hinton GE. Imagenet classification with deep convolutional neural networks. Advances in neural information processing systems, 2012. 1097-105.

22. Shelhamer E, Long J, Darrell T. Fully Convolutional Networks for Semantic Segmentation. IEEE Trans Pattern Anal Mach Intell. 2017;39(4):640-51.

23. Lerouge J, Herault R, Chatelain C, Jardin F, Modzelewski R. IODA: an Input/Output Deep Architecture for image labeling. Pattern Recognition. 2015;48(9):2847-58.

24. Tran PV. A fully convolutional neural network for cardiac segmentation in short-axis MRI. arXiv preprint arXiv:1604.00494. 2016.

25. Yamamuro M, Tadamura E, Kanao S, Wu YW, Tambara K, Komeda M, et al. Coronary angiography by 64-detector row computed tomography using low dose of contrast material with saline chaser: influence of total injection volume on vessel attenuation. J Comput Assist Tomogr. 2007;31(2):272-80.

26. Becker CR, Hong C, Knez A, Leber A, Bruening R, Schoepf UJ, et al. Optimal contrast application for cardiac 4-detector-row computed tomography. Invest Radiol. 2003;38(11):690-4.

27. Raff GL, Abidov A, Achenbach S, Berman DS, Boxt LM, Budoff MJ, et al. SCCT guidelines for the interpretation and reporting of coronary computed tomographic

연세대학교
YONSEI UNIVERSITY

angiography. J Cardiovasc Comput Tomogr. 2009;3(2):122-36.

28. Choi JH, Min JK, Labounty TM, Lin FY, Mendoza DD, Shin DH, et al. Intracoronary transluminal attenuation gradient in coronary CT angiography for determining coronary artery stenosis. JACC Cardiovasc Imaging. 2011;4(11):1149-57.

29. Kumar A, Bis KG, Shetty A, Vyas A, Anderson A, Balasubramaniam M, et al. Aortic root catheter-directed coronary CT angiography in swine: coronary enhancement with minimum volume of iodinated contrast material. AJR Am J Roentgenol. 2007;188(5):W415-22.

30. From AM, Bartholmai BJ, Williams AW, Cha SS, McDonald FS. Mortality associated with nephropathy after radiographic contrast exposure. Mayo Clin Proc. 2008;83(10):1095-100.

31. McCullough PA. Contrast-induced acute kidney injury. J Am Coll Cardiol. 2008;51(15):1419-28.

32. Rutty G, Saunders S, Morgan B, Raj V. Targeted cardiac post-mortem computed tomography angiography: a pictorial review. Forensic Sci Med Pathol. 2012;8(1):40-7.

33. Shetty AN, Bis KG, Vyas AR, Kumar A, Anderson A, Balasubramaniam M. Contrast volume reduction with superior vena cava catheter-directed coronary CT angiography: comparison with peripheral i.v. contrast enhancement in a swine model. AJR Am J Roentgenol. 2008;190(4):W247-54.

34. Choi JH, Koo BK, Yoon YE, Min JK, Song YB, Hahn JY, et al. Diagnostic

연세대학교
YONSEI UNIVERSITY

performance of intracoronary gradient-based methods by coronary computed tomography angiography for the evaluation of physiologically significant coronary artery stenoses: a validation study with fractional flow reserve. Eur Heart J Cardiovasc Imaging. 2012;13(12):1001-7.

35. Messenger JC, Casserly IP. Advances in contrast media and contrast injectors. Cardiol Clin. 2009;27(3):407-15.

36. Johnson LW, Lozner EC, Johnson S, Krone R, Pichard AD, Vetrovec GW, et al. Coronary arteriography 1984-1987: a report of the Registry of the Society for Cardiac Angiography and Interventions. I. Results and complications. Cathet Cardiovasc Diagn. 1989;17(1):5-10.

37. Lell MM, Jost G, Korporaal JG, Mahnken AH, Flohr TG, Uder M, et al. Optimizing Contrast Media Injection Protocols in State-of-the Art Computed Tomographic Angiography. Invest Radiol. 2014.

38. Taylor CA, Fonte TA, Min JK. Computational Fluid Dynamics Applied to Cardiac Computed Tomography for Noninvasive Quantification of Fractional Flow ReserveScientific Basis. Journal of the American College of Cardiology. 2013;61(22):2233-41.

39. Park HB, Heo R, o Hartaigh B, Cho I, Gransar H, Nakazato R, et al. Atherosclerotic plaque characteristics by CT angiography identify coronary lesions that cause ischemia: a direct comparison to fractional flow reserve. JACC Cardiovasc Imaging. 2015;8(1):1-10.

40. Park HB, Lee BK, Shin S, Heo R, Arsanjani R, Kitslaar PH, et al. Clinical

연세대학교
YONSEI UNIVERSITY

Feasibility of 3D Automated Coronary Atherosclerotic Plaque Quantification Algorithm on Coronary Computed Tomography Angiography: Comparison with Intravascular Ultrasound. Eur Radiol. 2015;25(10):3073-83.

41. Wada D, Nakamori Y, Yamakawa K, Fujimi S**.** First clinical experience with IVR-CT system in the emergency room: Positive impact on trauma workflow. Scandinavian Journal of Trauma, Resuscitation and Emergency Medicine. 2012;20:52-.

42. Shibui S, Tanaka M, Ino Y, Nomura K, Fujita T**.** Three-dimensional images by helical CT scan with intra-arterial injection of diluted contrast medium. Jpn J Clin Oncol. 1999;29(5):270-1.

43. Kim B-K, Cho I, Hong M-K, Chang H-J, Shin D-H, Kim J-S, et al. Usefulness of intraprocedural coronary computed tomographic angiography during intervention for chronic total coronary occlusion. American Journal of Cardiology. 2016;117(12):1868-76.

44. Achenbach S, Marwan M, Ropers D, Schepis T, Pflederer T, Anders K, et al. Coronary computed tomography angiography with a consistent dose below 1 mSv using prospectively electrocardiogram-triggered high-pitch spiral acquisition. European heart journal. 2010;31(3):340-6.

45. Min JK, Taylor CA, Achenbach S, Koo BK, Leipsic J, Norgaard BL, et al. Noninvasive Fractional Flow Reserve Derived From Coronary CT Angiography: Clinical Data and Scientific Principles. JACC Cardiovasc Imaging. 2015;8(10):1209-22.

연세대학교
YONSEI UNIVERSITY

46. Min JK, Leipsic J, Pencina MJ, Berman DS, Koo BK, van Mieghem C, et al. Diagnostic accuracy of fractional flow reserve from anatomic CT angiography. JAMA. 2012;308(12):1237-45.

47. Mowatt G, Cook JA, Hillis GS, Walker S, Fraser C, Jia X, et al. 64-Slice computed tomography angiography in the diagnosis and assessment of coronary artery disease: systematic review and meta-analysis. Heart. 2008;94(11):1386-93.

48. Budoff MJ, Dowe D, Jollis JG, Gitter M, Sutherland J, Halamert E, et al. Diagnostic performance of 64-multidetector row coronary computed tomographic angiography for evaluation of coronary artery stenosis in individuals without known coronary artery disease: results from the prospective multicenter ACCURACY (Assessment by Coronary Computed Tomographic Angiography of Individuals Undergoing Invasive Coronary Angiography) trial. J Am Coll Cardiol. 2008;52(21):1724-32.

49. Meijboom WB, Meijs MF, Schuijf JD, Cramer MJ, Mollet NR, van Mieghem CA, et al. Diagnostic accuracy of 64-slice computed tomography coronary angiography: a prospective, multicenter, multivendor study. J Am Coll Cardiol. 2008;52(25):2135-44.

50. Miller JM, Rochitte CE, Dewey M, Arbab-Zadeh A, Niinuma H, Gottlieb I, et al. Diagnostic performance of coronary angiography by 64-row CT. N Engl J Med. 2008;359(22):2324-36.

51. Park H, Heo R, ó Hartaigh B, Cho I, Gransar H, Nakazato R, et al. Atherosclerotic plaque characteristics by CT angiography identify coronary lesions that cause

연세대학교
YONSEI UNIVERSITY

ischemia: a direct comparison to fractional flow reserve. JACC. Cardiovascular imaging. 2015;8(1):1-10.

52. Dey D, Cheng VY, Slomka PJ, Nakazato R, Ramesh A, Gurudevan S, et al. Automated 3-dimensional quantification of noncalcified and calcified coronary plaque from coronary CT angiography. J Cardiovasc Comput Tomogr. 2009;3(6):372-82.

53. Nakazato R, Shalev A, Doh J-H, Koo B-K, Gransar H, Gomez MJ, et al. Aggregate plaque volume by coronary computed tomography angiography is superior and incremental to luminal narrowing for diagnosis of ischemic lesions of intermediate stenosis severity. Journal of the American College of Cardiology. 2013;62(5):460-7.

54. Dey D, Gaur S, Ovrehus KA, Slomka PJ, Betancur J, Goeller M, et al. Integrated prediction of lesion-specific ischaemia from quantitative coronary CT angiography using machine learning: a multicentre study. European Radiology. 2018.

55. Ronneberger O, Fischer P, Brox T**.** U-net: Convolutional networks for biomedical image segmentation. International Conference on Medical image computing and computer-assisted intervention, 2015. Springer: 234-41.

56. Çiçek Ö, Abdulkadir A, Lienkamp SS, Brox T, Ronneberger O**.** 3D U-Net: learning dense volumetric segmentation from sparse annotation. International Conference on Medical Image Computing and Computer-Assisted Intervention, 2016. Springer: 424-32.

57. Commandeur F, Goeller M, Betancur J, Cadet S, Doris M, Chen X, et al. Deep

연세대학교
YONSEI UNIVERSITY

Learning for Quantification of Epicardial and Thoracic Adipose Tissue from Non-Contrast CT. IEEE Transactions on Medical Imaging. 2018;PP(99):1-.

58. Zreik M, Lessmann N, van Hamersvelt RW, Wolterink JM, Voskuil M, Viergever MA, et al. Deep learning analysis of the myocardium in coronary CT angiography for identification of patients with functionally significant coronary artery stenosis. Medical image analysis. 2018;44:72-85.

59. Betancur J, Commandeur F, Motlagh M, Sharir T, Einstein AJ, Bokhari S, et al. Deep Learning for Prediction of Obstructive Disease From Fast Myocardial Perfusion SPECT. A Multicenter Study. 2018.

60. Dey D, Cheng VY, Slomka, PJ, Nakazato, R, Ramesh A, Gurudevan, S, Germano, Berman DS. Automated Three-dimensional Quantification of Non-calcified and Calcified Coronary Plaque from Coronary CT Angiography. Journal of Cardiovascular Computed Tomography. 2009:372-82.

61. Dey D, Schepis T, Marwan M, Slomka PJ, Berman DS, Achenbach S**.** Automated Three-dimensional Quantification of Non-calcified Coronary Plaque from Coronary CT Angiography: comparison with Intravascular Ultrasound Radiology. 2010;257(2):516-22.

62. Leipsic J, Abbara S, Achenbach S, Cury R, Earls JP, Mancini GBJ, et al. SCCT guidelines for the interpretation and reporting of coronary CT angiography: A report of the Society of Cardiovascular Computed Tomography Guidelines Committee. Journal of Cardiovascular Computed Tomography;8(5):342-58.

63. Agatston AS, Janowitz WR, Hildner FJ, Zusmer NR, Viamonte M, Detrano R**.**

연세대학교
YONSEI UNIVERSITY

Quantification of coronary artery calcium using ultrafast computed tomography. Journal of the American College of Cardiology. 1990;15(4):827-32.

64. Schuhbaeck A, Otaki Y, Achenbach S, Schneider C, Slomka P, Berman DS, et al. Coronary calcium scoring from contrast coronary CT angiography using a semiautomated standardized method. J Cardiovasc Comput Tomogr. 2015;9(5):446-53.

65. Mehta R, Sivaswamy J**.** M-net: A Convolutional Neural Network for deep brain structure segmentation. Biomedical Imaging (ISBI 2017), 2017 IEEE 14th International Symposium on, 2017. IEEE: 437-40.

66. He K, Zhang X, Ren S, Sun J**.** Delving deep into rectifiers: Surpassing human-level performance on imagenet classification. Proceedings of the IEEE international conference on computer vision, 2015. 1026-34.

67. Ioffe S, Szegedy C**.** Batch normalization: Accelerating deep network training by reducing internal covariate shift. International conference on machine learning, 2015. 448-56.

68. Srivastava N, Hinton G, Krizhevsky A, Sutskever I, Salakhutdinov R**.** Dropout: A simple way to prevent neural networks from overfitting. The Journal of Machine Learning Research. 2014;15(1):1929-58.

69. Hell MM, Dey D, Marwan M, Achenbach S, Schmid J, Schuhbaeck A**.** Non-invasive prediction of hemodynamically significant coronary artery stenoses by contrast density difference in coronary CT angiography. European Journal of Radiology;84(8):1502-8.

연세대학교
YONSEI UNIVERSITY

70. Hell MM, Motwani M, Otaki Y, Cadet S, Gransar H, Miranda-Peats R, et al. Quantitative global plaque characteristics from coronary computed tomography angiography for the prediction of future cardiac mortality during long-term follow-up. European Heart Journal - Cardiovascular Imaging. 2017;18(12):1331-9.

71. Motoyama S, Ito H, Sarai M, Kondo T, Kawai H, Nagahara Y, et al. Plaque Characterization by Coronary Computed Tomography Angiography and the Likelihood of Acute Coronary Events in Mid-Term Follow-Up. Journal of the American College of Cardiology. 2015;66(4):337-46.

연세대학교
YONSEI UNIVERSITY

Abstract (in Korean)

관상동맥 질환 평가를 위한 새로운 방법론:
새로운 영상 획득 기법부터 심층학습기반 자동 정량화까지

<지도교수 장혁재>

연세대학교 대학원 의과학과

홍영택

심혈관 질환은 여전히 세계에서 사망률의 주요 원인이다. 관상 동맥 단층 촬영 혈관 조영(CTA)은 관상 동맥 질환(CAD)의 진단을 위한 신뢰할 수 있는 비침습적 영상 모달리티로 자리 잡았다. 그러나 CAD의 진단-치료 현장 평가는 여전히 어려운 문제이다. 이 문제를 해결하기 위해, 이 논문은 새로운 영상 획득 기법에서부터 딥 러닝기반 자동 정량화까지 다룬다. 고품질 CTA를 얻기 위해 동물실험을 통해 도관 직접 주입방식의 선택적 CTA(S-CTA)를 개발했으며, CAD를 진단받은 환자에게 S-CTA의 임상적 타당성을 성공적으로 검증했다. 자동 정량화는 합성곱 신경망(CNN)을 이용해 개발했으며, 개발된 CNN모델은 최소 내강 면적, 직경 협착증 및 플라크 볼륨 등을 성공적으로 측정했습니다. S-CTA가 자동 정량화에 사용될 때 개발된 CNN은 종래의 CTA보다 더 나은

연세대학교
YONSEI UNIVERSITY

혈관 내강과 석회화 플라크의 본질적 특징을 성공적으로 분석할 수 있었다. S-CTA는 관상 동맥 혈관 조영 시스템과 CT 스캔을 함께하는 결합 시스템에서 시술 중 사용가능한 CTA방법으로 활용될 수 있습니다. S-CTA는 관상 동맥 중재시술 중 협착증에 대한 현장 평가 및 시술 전략 수립을 지원할 수 있습니다.

핵심 단어: 관상동맥 질환, 관상동맥 조영술, 컴퓨터 단층촬영, 딥 러닝, 영상 분할